Modulating the molybdenum coordination sphere of Escherichia coli trimethylamine N-oxide reductase

*Paul Kaufmann[1†], Benjamin R. Duffus[1†], Biljana Mitrova[1†], Chantal Iobbi-Nivol[2], Christian Teutloff[3], Manfred Nimtz[4], Lothar Jänsch[4], Ulla Wollenberger[1] and Silke Leimkühler[1]**

From the [1]Institute of Biochemistry and Biology, Department of Molecular Enzymology, University of Potsdam, 14476 Potsdam, Germany; [2]Aix-Marseille Université, CNRS, BIP UMR7281, 13402 Marseille, France; [3]Institute for Experimental Physics, Free University of Berlin, Arnimallee 14, 14195 Berlin, Germany; [4]Helmholtz Center for Infection Research, Inhoffenstraße 7, 38124 Braunschweig, Germany.

***corresponding author:**

Silke Leimkühler; Department of Molecular Enzymology, Institute of Biochemistry and Biology, University of Potsdam, Karl-Liebknecht-Str. 24-25, 14476 Potsdam, Germany; Tel.: +49-331-977-5603; Fax: +49-331-977-5128; E-mail: sleim@uni-potsdam.de

†These authors contributed equally to this work

Running title: Modulating the Mo coordination sphere of TMAO reductase

The abbreviations used are:

molybdenum cofactor (Moco)**,** molybdopterin (MPT)**,** bis-MPT guanine dinucleotide (bis-MGD)**,** trimethylamine *N*-oxide (TMAO), trimethylamine (TMA), dimethylsulfoxide (DMSO), formate dehydrogenase (FDH), xanthine dehydrogenase (XDH), with bis-MGD reconstituted TorA, (recTorA), didodecyldimethylammonium bromide (DDAB), iodoacetamide (IAA), guanosine-5'-triphosphate (5'GTP), guanosine monophosphate (GMP), high-performance liquid chromatography (HPLC), electron paramagnetic resonance (EPR), extended X-ray absorption fine structure (EXAFS), ethylenediaminetetraacetic acid (EDTA), *g*-factor (*g*), cyclic voltammetry (CV)

ABSTRACT

The well-studied enterobacterium *Escherichia coli* present in the human gut is able to reduce TMAO to trimethylamine (TMA) during anaerobic respiration. The TMAO reductase TorA is a monomeric, bis-molybdopterin guanine dinucleotide (bis-MGD) cofactor-containing enzyme belonging to the dimethylsulfoxide (DMSO) reductase family of molybdoenzymes. We report on a system for the *in vitro* reconstitution of TorA with molybdenum cofactors (Moco) from different sources. Higher TMAO reductase activities for TorA were obtained when using Moco-sources containing a sulfido ligand at the molybdenum atom. For the first time, we were able to isolate functional bis-MGD from *Rhodobacter capsulatus* formate dehydrogenase (FDH), which remained intact in its isolated state and after insertion into apo-TorA yielded a highly active enzyme. Combined characterizations of the reconstituted TorA enzymes by EPR spectroscopy and direct electrochemistry emphasize that TorA activity can be modified by changes in the Mo-coordination sphere. The combination of these results together with studies on amino acid exchanges at the active site led us to propose a novel model for substrate binding to the molybdenum atom of TorA.

INTRODUCTION

Escherichia coli is a facultative anaerobic bacterium that can adapt to many environmental conditions. In particular, *E. coli* can use several small compounds, including nitrate, dimethylsulfoxide (DMSO), or trimethylamine-N-oxide (TMAO), as alternative electron acceptors to produce energy.[1-3] Under oxygen limitation, TMAO can be used as terminal electron acceptor for energy production with a standard redox potential (pH 7.0) for the TMAO/TMA couple of +130 mV. [3, 4] In *E. coli*, the operon composed of the genes *torCAD* encodes for the proteins of the TMAO reductase system, the expression of which is controlled by the presence of TMAO.[5-7] However, in contrast to other alternative respiratory systems, the expression of TMAO reductase is not repressed by the presence of oxygen.[5] Instead, in aerobically grown cells, the activity of TMAO reductase was reported to be largely reduced down to 5% as compared to anaerobically grown cells.[8] Here, a postranslational inactivation has to occur, since the protein levels were not reduced under aerobic conditions. [19]

The *E. coli* TMAO reductase complex faces the periplasm and consists of the molybdenum cofactor (Moco)-containing terminal reductase TorA responsible for substrate-binding/conversion and the membrane-associated *c*-type cytochrome TorC, which uses a menaquinol or demethylmenaquinol as electron donor.[5, 9, 10] TorA contains the form of Moco typical for the dimethylsulfoxide (DMSO) reductase family of molybdoenzymes, which is composed as a bis-molybdopterin guanine dinucleotide (bis-MGD).[11] Enzymes of this family, which are only present in prokaryotes, fulfill important physiological functions by playing vital roles in the global nitrogen and carbon cycles and in the detoxification of species such as arsenite, selenite or chlorate.[12] In almost all cases, the enzymes catalyze reactions that involve two-electron oxidation-reduction chemistry coupled to the transfer of an oxygen and two protons to form

water, or the reverse reaction.[13]

DMSO reductase family enzymes were revealed to display a diverse coordination environment at the molybdenum atom.[14] In enzymes like e.g. nitrate reductase, DMSO reductase or formate dehydrogenase (FDH) the molybdenum coordination sphere encompasses the four sulfur atoms from the two dithiolene groups of the pyranopterin rings and further an oxo- or sulfido group as fifth ligand and a sixth ligand usually represented by an amino acid from the protein backbone being a serine, a cysteine, a selenocysteine, or an aspartate.[15-18] However, a hydroxide and/or water molecule has also been identified to be present in arsenite oxidase.[12, 19] The X-ray absorption fine structure data of TorA resulted in the interpretation of the molybdenum coordination sphere of TorA containing four dithiolene sulfur ligands, one serine-oxygen ligand and a oxo-/hydroxo-/water-ligand or oxygen atom.[20]

Since expression studies showed that the protein levels of TorA remained constant during aerobic and anaerobic growth while enzyme activity was reduced down to 5%, we investigated the effect of oxygen on TorA activity in more detail.[8, 21] Here, we show that under anaerobic conditions the molybdenum coordination environment of TorA contains a sulfido ligand, which is lost during aerobic purification of the enzyme. In particular, by *in vitro* reconstitution of apo-TorA with Moco's from different sources we showed that higher activities of TorA were gained when a terminal sulfido ligand was present at the cofactor. Investigations by direct electrochemistry showed a catalytic current only with sulfido-ligand containing TorA enzyme variants. Furthermore, we were able to isolate and insert functional bis-MGD into apo-TorA to yield active enzyme, extracted from Mo=S/bis-MGD containing FDH as source enzyme. By substituting the active site serine 191 to a cysteine in combination with alkylation of this introduced amino acid, we demonstrated that the cysteine is not required as a ligand to the molybdenum atom during

catalysis. The combination of the results of this study led us to propose a Mo coordination sphere of TorA in which a sulfido- rather than an oxo-ligand is present, resulting in a novel model for substrate binding.

EXPERIMENTAL PROCEDURES

Expression and Purification conditions.

Apo-TorA (from pJF119EH[22]), MobA (from pCT800A[23]), and TorD (from pET28TorD[22]) were expressed and purified as described previously with slight modifications. Site directed mutagenesis of TorA was performed using the Agilent QuikChangeLightning Kit. Moco-containing TorA wild type and TorA-S191C were expressed in *E. coli* BW25113 cells. For expression under aerobic conditions, the main culture was inoculated with aerobically grown preculture (12h, 37°C and 220 rpm) in a 1:500 dilution. The main culture was supplemented with 20 μM isopropyl β-D-1-thiogalactopyranoside (IPTG) and ampicillin (150 μg/mL) and grown for 24h at 30°C and 130 rpm under aerobic conditions. For expression under anaerobic conditions, precultures were supplemented with ampicillin (150 μg/mL) and grown aerobically (12h, 37°C and 220 rpm). The main culture was inoculated with preculture in a 1:10 dilution and supplemented with 70 μM IPTG, 1 mM molybdate, ampicillin (150 μg/mL) and 7 mM TMAO. For anaerobic expression, cultures were grown in closed flasks at 37°C for 30h. Expression of XDH or $XDH^{desulfo(\Delta XdhC)}$ was carried out as described previously.[24, 25]

After harvesting of cells and cell lysis, the cleared lysate was applied to 0.3-0.5 mL of Ni-nitrilotriacetate (Ni-NTA, Macherey & Nagel, Düren, Germany) resin per Liter of cell culture, depending on the growth conditions. For purification of anaerobically expressed TMAO reductase under aerobic conditions ($-O_2^{ex}/+O_2^{pur}$) 0.3 mL of Ni-NTA per liter of *E. coli* was used.

The loaded resin was washed with 20 column volumes of 50 mM NaH_2PO_4 buffer, 10 mM and 20 mM imidazole each. Elution of the proteins was achieved with buffer containing 250 mM imidazole. For purification of anaerobically expressed TMAO reductase, cells of anaerobic cultures were split into two fractions after harvesting. One fraction was subjected to aerobic purification ($-O_2^{ex}/+O_2^{pur}$) as described above and the other fraction was transferred into the glove box (Coy Laboratory Products, Grass Lake, MI) and allowed to rest for at least 2h to become anaerobic ($-O_2^{ex}/-O_2^{pur}$). Cell lysis was carried out by sonication (HUT SONI130, G. Heinemann, Schwäbisch Gmünd, Germany) followed by Ni-NTA chromatography including all purification-steps described for aerobic purification.

R. capsulatus FDH and XDH were purified as described previously.[25, 26] Proteins were transferred into storage buffer using PD-10 columns (GE Healthcare, Piscataway, NJ). All proteins except for FDH were stored in Tris-HCl, pH 7.2. FDH was stored in 75 mM potassium phosphate, 10 mM azide, pH 7.5.

Cofactor analysis.

Metal analysis was performed using PerkinElmer (Waltham, MA) Life Sciences Optima 2100DV inductively coupled plasma optical emission spectrometer as described earlier.[27] The bis-MGD cofactor was detected fluorometrically after its conversion to FormA-GMP with slight modifications.[28] 200 µL of pure protein solution (5 to 10 µM) in 100 mM Tris-HCl, pH 7.2 were oxidized by the addition of 25 µL acidic iodine and incubated over night at room temperature. Excess of iodine was removed by addition of 27.5 µL 1% ascorbic acid and pH was adjusted to 8.3 by addition of 100 µL 1M Tris. Separation of the FormA-GMP fraction was carried out using a C18 reversed phase HPLC column (4.6 * 250 mm ODS Hypersil (Thermo Fisher, particle size

5 µm) equilibrated in 5 mM ammonium acetate and 15% (v/v) methanol. Detection of FormA-GMP during elution was carried out using an Agilent 1100 series fluorescence detector (excitation at 383 nm, emission at 450 nm).

Enzyme assays.

TMAO reductase activity was measured under anaerobic conditions in a volume of 1 mL following the oxidation of pre-reduced benzyl viologen at 600 nm. The activity assay contained 40 mM benzyl viologen and 7.5 mM TMAO as substrate in 100 mM Sorenson's phosphate buffer, pH 6.5. Benzyl viologen reduction was achieved by addition of sodium dithionite until $OD_{600\ nm}$=1 was reached. Measurement was started by addition of 0.2 µg to 2 µg of TorA. The activity was calculated using the equation U = 0.5 x (ΔAbs_{600}/min)/ ε_{600}(benzyl viologen)/V, using the extinction coefficient for benzyl viologen of 7.4 $mmol^{-1}$ x cm^{-1}. One Unit is defined as the reduction of 1 µmol TMAO per minute.

Apo-TorA reconstitution assays.

For *in vitro* apo-TorA reconstitution, *R. capsulatus* XDH wild type or XDH expressed in the absence of XdhC ($XDH^{desulfo(\Delta XdhC)}$) was used as Moco source. For Moco extraction from these enzymes, 30 µM of proteins were incubated at 95 °C for 4 minutes in a total volume of 400 µL. After centrifugation, the supernatant was used as Moco source. Reconstitution mixtures were incubated at 37 °C for 7 h and contained 1.3 µM apo-TorA, 2 µM TorD, 2 µM MobA, 1 mM 5'GTP and 1 mM $MgCl_2$ and 200 µL Moco-containing supernatant in 100 mM Tris-HCl, pH 7.2. For apo-TorA reconstitution with Moco extracted from *R. capsulatus* FDH (sulfido-containing bis-MGD), 1.3 µM apo-TorA were mixed with 200 µL supernatant of 30 µM heat denatured

FDH in 100 mM Tris-HCl, pH 7.2. The reconstitution assay was incubated at 37 °C for 7 h. All steps of Moco extraction and TorA reconstitution were carried out under anoxic conditions in a glove box (Coy Laboratory Products, Grass Lake, MI). After incubation, reconstituted TorA was purified from the mixtures by gel filtration on a Superdex200 10/300GL column (GE Healthcare). TorA containing fractions were combined and used for further assays.

Cyanide treatment and chemical sulfuration of proteins.

Desulfuration of XDH was achieved after incubation with 10 mM potassium cyanide for at least 3h at room temperature. Released thiocyanate was removed by gel filtration using PD-10 columns (GE Healthcare). For chemical sulfuration of XDH, 1 mL of protein was treated under anaerobic conditions with 10 µL of 2.5 mM methyl viologen, 20 µL of 100 mM Na_2S and sodium dithionite until a slight blue color of the solution appeared due to reduction of methyl viologen. The sulfuration assay was incubated at room temperature for 30 minutes. Afterwards XDH was desalted using PD-10 columns (GE Healthcare).

Carboxamidomethylation of TorA and TorA-S191C.

TorA and TorA-S191C samples (5.04 µM in 100 mM, pH 7.2) were incubated with 1 mM iodoacetamide (IAA) in the presence or absence of 7.5 mM TMAO for 150 minutes in a total volume of 500 µL. Afterwards all samples were applied to gel filtration (Nick columns, GE Healthcare) to remove unbound TMAO and/or IAA. Control proteins were treated with the same volume of 100 mM Tris-HCl buffer instead of TMAO or IAA. The eluted proteins were concentrated using ultracentrifugation devices (Amicon Ultra, 10 kDa cutoff) to a final volume of 50 µL. The concentrated samples were applied to denaturing SDS-PAGE (16 µg protein per

lane). After Coomassie staining, gel bands corresponding to TorA were cut and dried using the vacuum centrifuge for 45 minutes at 37 °C.

LC-MS/MS.

After SDS-PAGE gel pieces containing the TorA subunit were reduced using 50 µL of 50 mM TCEP for 1 h at 60 °C followed by alkylation with 30 µL of 200 mM methyl methanethiosulfonate (MMTS) for 10 minutes at RT, and in-gel digestion with trypsin overnight at 37 °C (Promega, USA). Obtained peptides were extracted and purified with reversed-phase C18 ZipTips (Millipore, USA). LC-MS/MS analyses of desalted peptides were performed on a Dionex UltiMate 3000 n-RSLC system connected to an Orbitrap Fusion™ Tribrid™ MS (Thermo Scientific, Dreieich, Germany). Peptides were loaded onto a C_{18} pre-column (3 µm RP18 beads, Acclaim, 75 µm x 20 mm), washed for 3 minutes at a flow rate of 6 µL/min and separated on a C_{18} analytical column (3-µm, Acclaim PepMap RSLC, 75 µm x 50 cm, Dionex) at a flow rate of 200 nL/min via a linear 60 minute gradient from 97% buffer A (buffer A = 0.1% formic acid in water) to 25% B (buffer B = 0.1% formic acid in 80% acetonitrile), followed by a 15 minute gradient from 25% buffer B to 62% buffer B. The effluent was electro-sprayed by a stainless steel emitter (Thermo Scientific). The mass spectrometer was controlled and operated in the data-dependent mode using the Xcalibur software allowing the automatic selection of 2-4 fold charged peptides and their subsequent fragmentation (top speed mode) using the ion routing multipole with nitrogen as collision gas (HCD) and orbitrap detection (resolution 15 K). Every 3 seconds a MS survey scan was performed (resolution 120 K). The maximum collection time for peptides was set to 200 ms. Dynamic exclusion was set to 6 seconds. MS/MS raw data files were processed via the Proteome Discoverer program Version 1.4 (Thermo Scientific) on a Mascot

server (V. 2.3.02, Matrix Science) using the NCBI database. The following search parameters were used: enzyme, trypsin; maximum missed cleavages: 1, variable modifications: methyl methanethiosulfonate MMTS (C) and carboxamidomethyl CAM (C); peptide tolerance, 10 ppm; MS/MS tolerance, 0.03 Da. For relative quantification of peptides of interest, ion traces of the respective molecular ions with a mass tolerance of 10 ppm were used.

Electrochemistry.

The electrochemical experiments were carried out in a lab-built three-electrode cell with a total volume of 1 mL, employing a platinum wire as counter electrode, an Ag/AgCl, 1 M KCl reference electrode (Microelectrodes Inc.; Bedford, NH, USA) against which all potentials are reported, and a modified graphite rod working electrode (Alfa Aesar; Karlsruhe, Germany). All the experiments were performed at room temperature in a glovebox under anaerobic conditions (minimum of 2% H_2 and 98% N_2) with PalmSens potentiostat and analyzed with PSLite 4.8 software (Pamlsens, The Netherlands) and OriginPro 2016.

Electrode modification.

A graphite rod electrode with a diameter of 3.5 mm was cleaned on emery paper with two different grain sizes and afterwards ultrasonicated for 20 s and dried under N_2 stream. The cleaned electrode was modified with a mixture of 1:1 volume ratio of 2 mM didodecyldimethylammonium bromide (DDAB) and TorA variants. For the direct bioelectrocatalysis different concentrations of TorA were used, dependent on the Moco saturation in the enzyme. A 6 μL aliquot of this mixture was drop-casted on the electrode surface and left to dry in a desiccator at 4 °C for 15-20 minutes. The electrode was then transferred to the anaerobic

glovebox and used for the experiments. The measurements of the bioelectrocatalysis were always performed under conditions of saturated substrate concentration and constant stirring of the cell solution to prevent substrate-limited conditions.

The mediated electrochemistry was performed in the presence of 1 mM methyl viologen as a mediator and the modification and substrate concentration were kept the same as for the unmediated electrochemistry. During the modification, the concentration of the enzyme variants applied to the electrode surface was kept constant (290 μM). Chronoamperometry was performed at $E_{applied}$ = -0.8 V. The value of the catalytic current was measured as difference of the stationary currents of the I/t-curve before and after addition of TMAO. The onset potential was deduced from CV trace where the current rises over the background charging current.

EPR Preparative and Spectroscopic Methods.

EPR samples were prepared either aerobically in an ice bath or anaerobically in a Coy Chamber at O_2 levels < 10 ppm at 4 °C in a thermoblock, in 100 mM Tris, pH 7.2. Typical sample preparation methods involved excess addition of freshly-prepared sodium dithionite (10 mM) or potassium ferricyanide (10 mM) to as-isolated (non-reconstituted) or as-obtained (reconstituted) TorA samples (100 μM) that were then immediately frozen in a liquid nitrogen-cooled ethanol bath before complete freezing in liquid nitrogen. Where applicable, as-isolated and as-obtained samples were prepared by simple buffer dilution of the enzyme, followed by sample freezing. Redox-cycled TorA-WT samples were prepared analogously to the methods reported previously for TMAO reductase, as part of purification methods with minor procedural alterations.[20, 29]

CW X-Band EPR spectra recorded at 9.4 GHz were obtained using a home-built spectrometer (microwave bridge, ER041MR, Bruker, Rheinstetten, Germany; lock-in amplifier, SR810,

Stanford Research Systems, Stanford, CA, USA; microwave counter, 53181A, Agilent Technologies) equipped with a Bruker SHQ resonator. An ESR 910 helium flow cryostat with an ITC503 temperature controller (Oxford Instruments, Oxfordshire, UK) was used for temperature control. CuEDTA was used as a standard reference with respect to spin quantitation. Field corrections were performed as needed by measuring a standard solution of sodium dithionite-reduced sample of *R. capsulatus* formate dehydrogenase[26] (100 μM) at 80 K under acquisition conditions identical to those reported herein, and correcting with respect to the [2Fe-2S] clusters present. At this temperature, the [2Fe-2S] clusters present are nearly identical to those reported for *C. necator* formate dehydrogenase[30]. Baseline subtraction was performed relative to a buffer blank at the reported temperature. Spin quantitation was performed using the utility 'spincounting' (http://lcts.github.io/spincounting/) in Matlab (Mathworks; Natick, MA, USA) with associated tune pictures that measured the sample Q-factor. CuEDTA standards of known concentration that were ran on the same day of measurement to estimate the associated spectrometer transfer-factor. Simulation of EPR data, where applicable was performed with the EasySpin toolbox[31] in Matlab and yielded the *g*-values and associated parameters reported.

RESULTS

Comparison of aerobically and anaerobically expressed TorA suggests the presence of a sulfido ligand in the Mo coordination sphere.

To investigate the effect of oxygen on the assembly of TorA, we recombinantly expressed *torAD* under aerobic ($+O_2^{ex}$) and anaerobic ($-O_2^{ex}$) conditions in the presence of 7 mM TMAO and characterized the enzymes that were purified either under aerobic ($+O_2^{pur}$) or anaerobic ($-O_2^{pur}$) conditions (Figure 1).

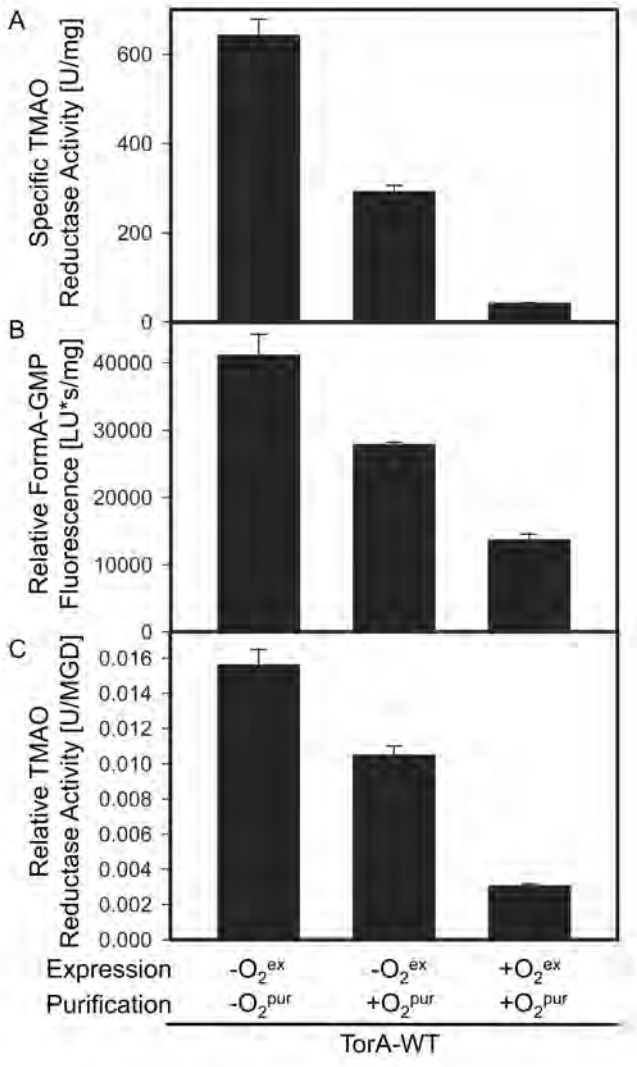

Figure 1: **The effect of oxygen on the TMAO reductase activity of TorA.**

TorA was expressed and purified either aerobically ($+O_2$) or anaerobically ($-O_2$), respectively, as described under Materials and Methods. (A) Specific activity of TorA at 30°C in U/mg (µmol of TMAO reduced per minute and mg of enzyme). (B) Relative FormA-GMP fluorescence of bis-MGD released from TorA. The bis-MGD cofactor was oxidized to FormA-GMP and quantified after separation on a C18-RP column. Integrated FormA-GMP peak-areas were related to the amount of protein in mg. (C) Relative TMAO reductase activities (U/MGD) in µmol TMAO reduced per MGD present in the protein (calculated as specific activities (U/mg) shown in panel A divided by relative fluorescence values in (LU/mg) in panel B).

The specific activity of the aerobically expressed and purified ($+O_2^{ex}/+O_2^{pur}$) enzyme was largely reduced to 5% compared to the anaerobically expressed and purified ($-O_2^{ex}/-O_2^{pur}$) enzyme (Figure 1A). The reduced activity can only be partially explained by a reduced bis-MGD content, since the detected MGD (as FormA-GMP) was 30% relative to the completely anaerobically prepared sample (Figure 1B). We related the enzyme activity to the amount of FormA-GMP detected in the enzyme instead to using the molybdenum content, since we observed unspecific molybdate binding to TorA preparations. Since also unspecific GMP binding was observed, detected FormA-GMP should refer only to specifically bound bis-MGD to the enzyme.[32-34] The aerobically prepared sample showed 20% of the activity/bis-MGD as detected for the anaerobically prepared enzyme (Figure 1C). Surprisingly, when the anaerobically expressed enzyme was purified under aerobic conditions ($-O_2^{ex}/+O_2^{pur}$), a similar loss of activity in addition to a reduced MGD content was observed (Figure 1A + B). When relating the specific activity to the MGD content, the aerobically purified enzyme ($-O_2^{ex}/+O_2^{pur}$) had a reduced relative activity of 25% as compared to the enzyme purified under anaerobic conditions ($-O_2^{ex}/-O_2^{pur}$) (Figure 1C), showing an inactivation of the enzyme by oxygen.

To determine the basis of the differences in activity in the aerobically and anaerobically prepared enzymes, we analyzed the impact of different ligands at the Mo coordination sphere on TorA activity. Here, we made use of the established *in vitro* reconstitution system for apo-TorA with *in vitro* synthesized bis-MGD, which enabled us to use different forms of Mo-MPT as initial cofactor source.[33] The bis-MGD free form of TorA can be obtained from a Moco-deficient *E. coli* strain (see experimental procedures). This assay solely consists of purified MobA, Mg-GTP and extracted Moco from an enzyme source (i.e. xanthine dehydrogenase (XDH) or sulfite oxidase) in

addition to apo-TorA and TorD.[33, 35] While the reconstitution of TorA is performed under anaerobic conditions, TorA is subsequently purified from the reconstitution mixture under aerobic conditions, so that the obtained activities of the reconstituted enzymes consequently were compared to the activities of the TorA-WT ($-O_2^{ex}$/$-O_2^{pur}$) enzyme (which was set to 100% activity in Figure 2 for better comparability).

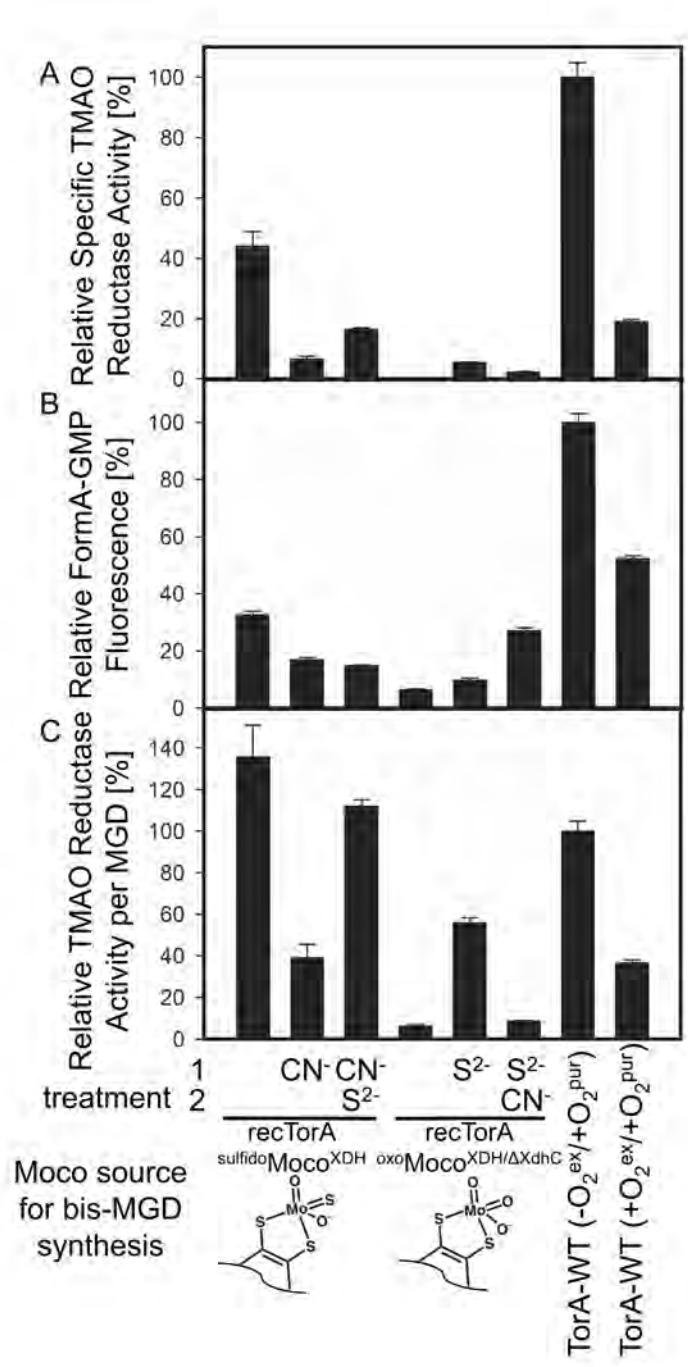

Figure 2: **The activity of TorA after reconstitution with different cofactors.**

(A) Relative activities of TorA-WT or reconstituted apo-TorA with different cofactors at 30°C in U/mg (µmol of TMAO reduced per minute and mg of enzyme). The activities were normalized to anaerobically expressed and aerobically purified TorA-WT ($-O_2^{ex}/+O_2^{pur}$) (shown in Figure 1) set to an activity of 100%. Reconstitution of 1.3 µM apo-TorA was carried out under anaerobic

conditions by incubation with 2 µM MobA, 200 µl of the respective isolated Mo-MPT forms in the presence of 1 mM GTP, 1 mM $MgCl_2$, and 2 µM TorD. Gel filtration was performed under aerobic conditions to separate TorA from the reconstitution mixture. (B) Relative FormA-GMP fluorescence of bis-MGD released from TorA. The bis-MGD cofactor was oxidized to FormA-GMP and quantified after separation on a C18-RP column. Integrated FormA-GMP peak-areas were related to the amount of protein in mg. Relative FormA-GMP fluorescence (LU*s/mg) was normalized to anaerobically expressed and aerobically purified TorA-WT set to 100%. (C) Relative TMAO reductase activities (U/MGD) in µmol TMAO reduced per MGD present in the protein (calculated as relative activities (U/mg) shown in panel A divided by relative fluorescence values in (LU/mg) in panel B). The obtained values were normalized to anaerobically expressed and aerobically purified TorA-WT ($-O_2^{ex}/+O_2^{pur}$) set to 100%.

To study the influence of a sulfur ligand in the Mo coordination sphere on TorA activity, we extracted the sulfido-containing Moco from *Rhodobacter capsulatus* XDH, which can be produced in a 100%-loaded form with the Mo=S ligand.[36, 37] Using this Mo=S containing Moco, the TorA activities showed a saturation of reconstitution after about 5 h (data not shown), consistent with the data reported before using sulfite oxidase as Moco source.[33] When the source XDH contained an oxo ligand in place of the sulfido ligand, which was removed by treatment with KCN prior to reconstitution, a reduced relative TorA activity was obtained (Figure 2A-C). To assess whether the impaired activity is indeed based on the sulfido ligand, the inactive cyanide-treated desulfo XDH was chemically resulfurated.[38] The results in Figure 2C show that TorA activities were obtained with a comparable activity to the untreated XDH. Further, the obtained activities after 7 h of reconstitution were related to their determined relative MGD contents. The results in Figure 2C show that the highest relative activity per MGD was obtained for reconstituted TorA with native XDH containing the sulfido ligand as Moco source.

To verify these results, we used an additional XDH as unsulfurated Mo=O source that was expressed in the absence of XdhC (referred to as $^{oxo}Moco^{XDH/\Delta XdhC}$), known to be the chaperone essential for Moco sulfuration.[39] TorA reconstituted with Moco extracted from this enzyme resulted in an almost inactive enzyme (Figure 2). When the Moco of $XDH^{\Delta XdhC}$ was chemically sulfurated before extraction, TorA activity was regained. In contrast, when the chemically sulfurated Moco from $XDH^{\Delta XdhC}$ was treated with cyanide, a TorA activity similar to the one reconstituted with non-sulfurated $XDH^{\Delta XdhC}$ was obtained (Figure 2).

The results overall indicate that TorA activity depends on the presence of a sulfido ligand at the bis-MGD cofactor. The presence of the sulfido ligand thereby is influenced when oxygen is present during purification.

Reconstitution of TorA with isolated bis-MGD cofactor.

A coordination sphere with a sulfido ligand at the molybdenum atom has been reported also for other molybdoenzymes from the DMSO reductase family like nitrate reductase or FDH[15, 16, 40]. For the first time, a direct reconstitution approach was attempted of an enzyme with an extracted bis-MGD cofactor from an enzyme source. Here, we were using *Rhodobacter capsulatus* FDH (*Rc*FDH) as bis-MGD source enzyme, in which the extracted cofactor after heat denaturation was directly inserted into apo-TorA without the aid of MobA or TorD (Figure 3A-C).

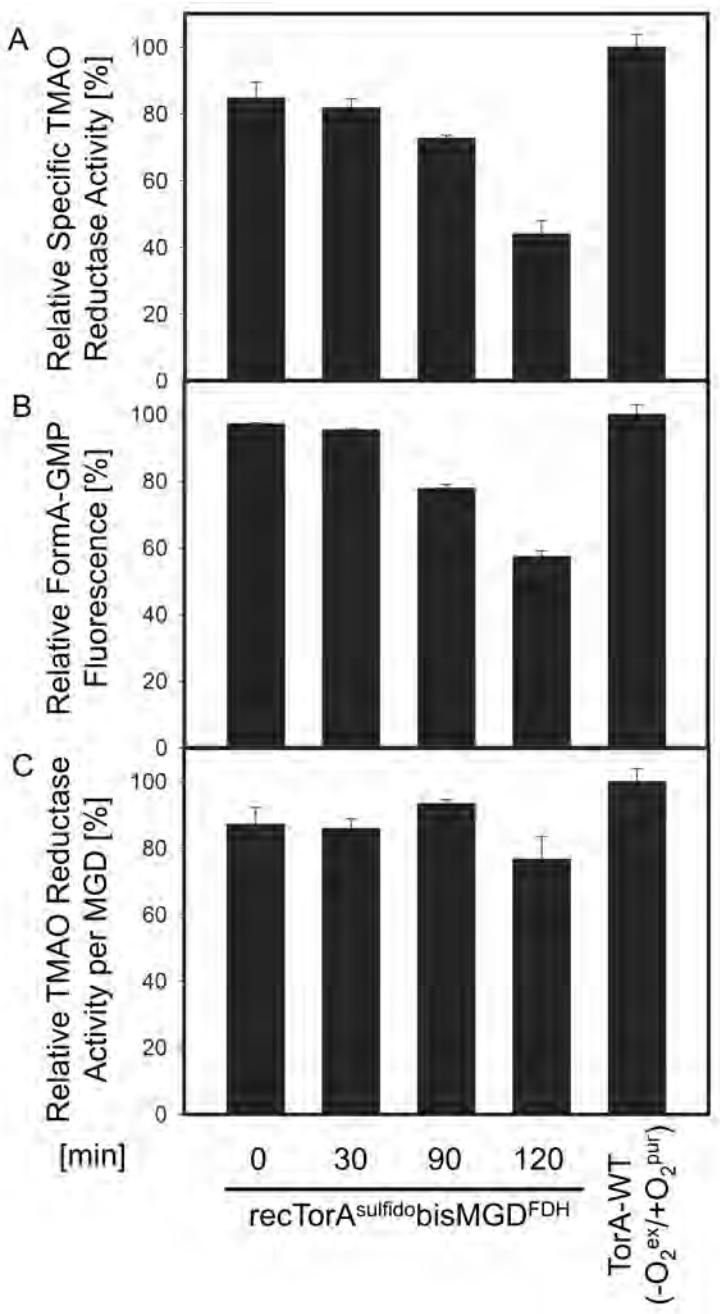

Figure 3. **The activity of TorA after reconstitution with sulfido-containing bis-MGD cofactor extracted from FDH.**

(A) The activity of reconstituted TorA with extracted sulfido-containing bis-MGD from *R. capsulatus* FDH. Extracted bis-MGD was incubated under anaerobic conditions for 0, 30, 90 or 120 minutes as indicated before the addition of apo-TorA. The activities were normalized to anaerobically expressed and aerobically purified TorA-WT ($-O_2^{ex}/+O_2^{pur}$) (shown in Figure 1) set

to an activity of 100%. (B) Relative FormA-GMP fluorescence of bis-MGD released from TorA after reconstitution. The bis-MGD cofactor was oxidized to FormA-GMP and quantified after separation on a C18-RP column. Integrated FormA-GMP peak-areas were related to the amount of protein in mg. Relative FormA-GMP fluorescence (LU*s/mg) was normalized to anaerobically expressed and aerobically purified TorA-WT set to 100%. (C) Relative TMAO reductase activities (U/MGD) in µmol TMAO reduced per MGD present in the protein (calculated as relative activities (U/mg) shown in panel A divided by relative fluorescence values in (LU/mg) in panel B). The obtained values were normalized to anaerobically expressed and aerobically purified TorA-WT set to 100%.

With this direct reconstitution procedure active TorA was obtained, showing for the first time that the bis-MGD cofactor remained intact outside of the protein. Analysis of the stability of extracted bis-MGD showed that the cofactor was stable for 90 minutes after extraction under anaerobic conditions, before a decrease in reconstitution efficiency was observed (Figure 3). Overall, comparable normalized relative activities of bis-MGD reconstituted TorA were obtained as compared to purified TorA-WT ($-O_2^{ex}/+O_2^{pur}$) (Figure 3C).

The S191C variant of E. coli TMAO reductase performs TMAO reduction.

The crystal structure of *Shewanella massilia* TMAO reductase has revealed a serine residue from the protein backbone as a ligand to the molybdenum in TorA.[11] Since *R. capsulatus* FDH[40] and the *E. coli* nitrate reductase NapA[15] likewise contain an active site cysteine ligand, we set out to analyze the influence of the Mo-ligating serine-to-cysteine substitution of the anaerobically expressed TorA-S191C variant.

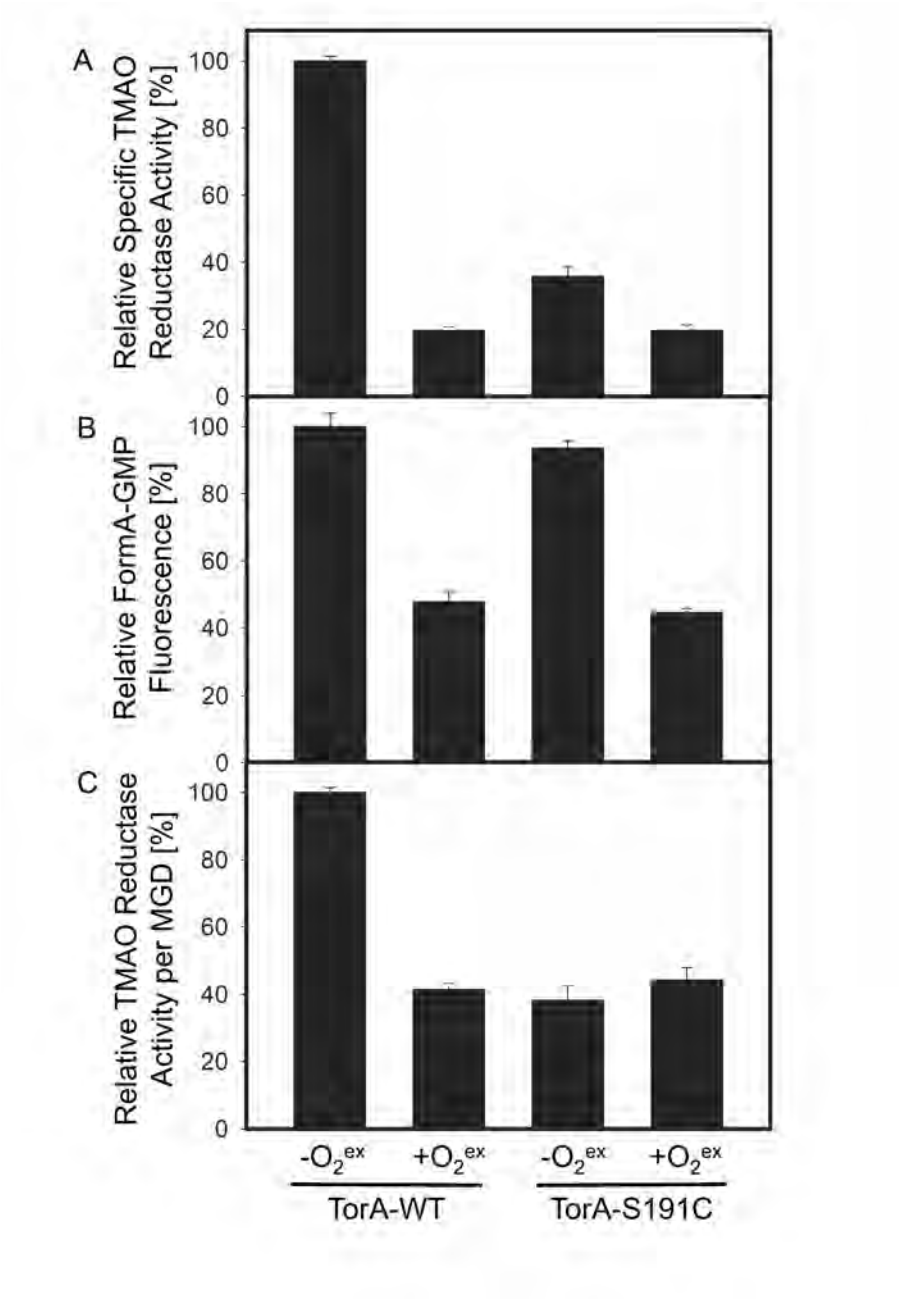

Figure 4: **Activities of the TorA-S191C variant expressed under aerobic and anaerobic conditions.**

(A) Relative activities of TorA-WT in comparison to the TorA-S191C variant at 30°C in U/mg (µmol of TMAO reduced per minute and mg of enzyme). The activities were normalized to anaerobically expressed and aerobically purified TorA-WT ($-O_2^{ex}/+O_2^{pur}$) (shown in Figure 1) set to an activity of 100%. (B) Relative FormA-GMP fluorescence of bis-MGD released from TorA after reconstitution. The bis-MGD cofactor was oxidized to FormA-GMP and quantified after

separation on a C18-RP column. Integrated FormA-GMP peak-areas were related to the amount of protein in mg. Relative FormA-GMP fluorescence (LU*s/mg) was normalized to anaerobically expressed and aerobically purified TorA-WT set to 100%. (C) Relative TMAO reductase activities in µmol TMAO reduced per MGD present in the protein. The obtained values were normalized to anaerobically expressed and aerobically purified TorA-WT set to 100%.

As shown in Figure 4, the TorA-S191C ($-O_2^{ex}/+O_2^{pur}$) variant was active with a relative activity of 38% of TorA-WT expressed under identical expression and purification conditions. The amino acid exchange had no influence on the bis-MGD insertion into the enzyme, however, when the activity was related to the bis-MGD content, TorA-S191C expressed under anaerobic conditions showed only 40% of the activity as compared to anaerobically expressed TorA-WT (Figure 4A-C). Surprisingly, the TorA-S191C variant expressed and purified under aerobic conditions ($+O_2^{ex}/+O_2^{pur}$) was as active as the corresponding wild-type protein prepared under the same conditions (Figure 4 C).

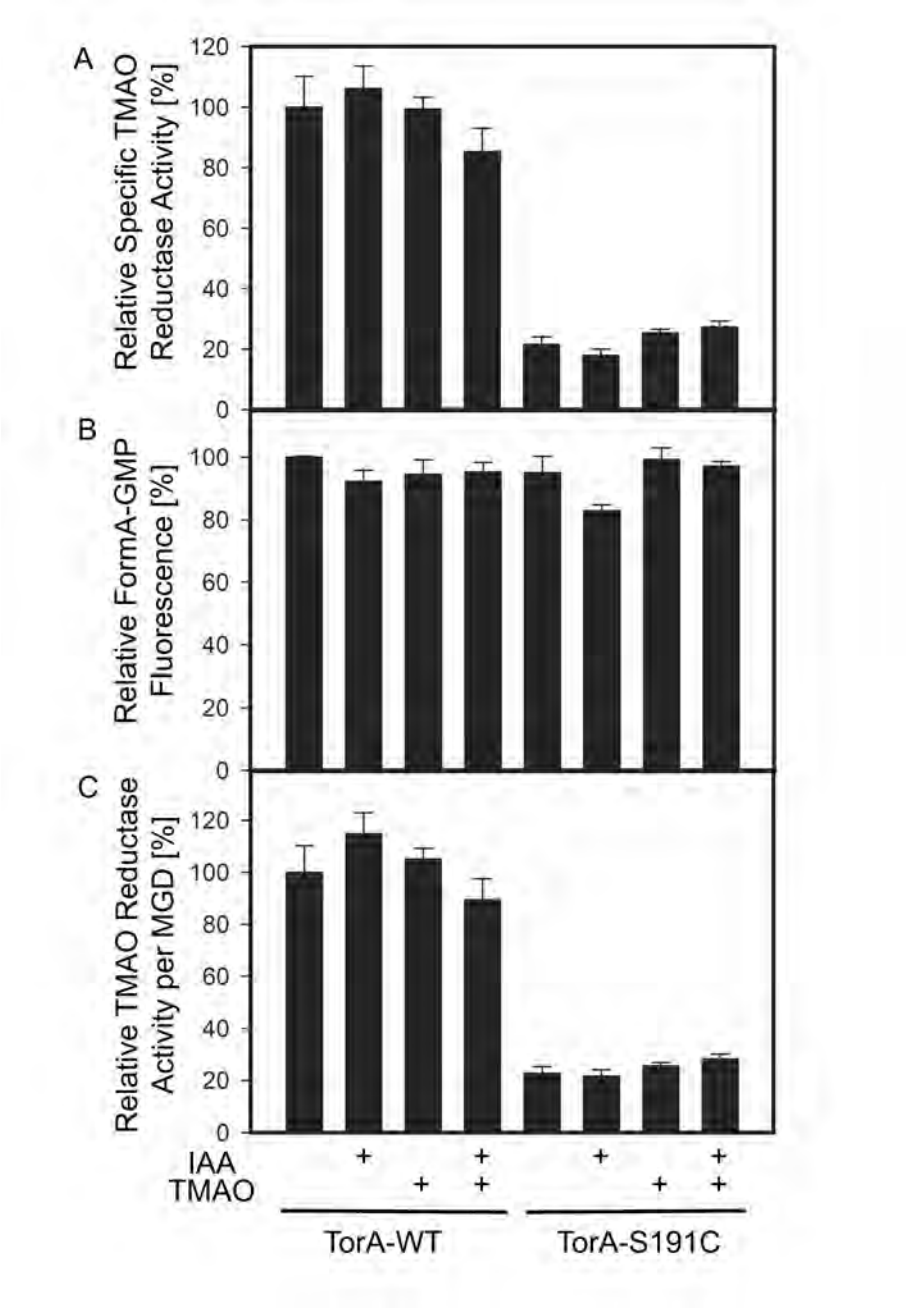

Figure 5: **Influence of iodoacetamide on the active-site cysteine in the TorA-S191C variant.** (A) 5 µM of TorA-WT or TorA-S191C were incubated with either 1 mM IAA, 7.5 mM or TMAO as indicated in a total volume of 500 µl for 2.5 hours at room temperature. Afterwards unbound reagents were removed using Nick columns (GE). Relative activities of IAA-treated TorA-WT and variant TorA-S191C at 30°C in U/mg (µmol of TMAO reduced per minute and mg of enzyme). The activities were normalized to anaerobically expressed and aerobically purified TorA-WT ($-O_2^{ex}/+O_2^{pur}$) (shown in Figure 1) set to an activity of 100%. (B) Relative

FormA-GMP fluorescence of bis-MGD released from TorA after reconstitution. The bis-MGD cofactor was oxidized to FormA-GMP and quantified after separation on a C18-RP column. Integrated FormA-GMP peak-areas were related to the amount of protein in mg. Relative FormA-GMP fluorescence (LU*s/mg) was normalized to anaerobically expressed and aerobically purified TorA-WT set to 100%. (C) Relative TMAO reductase activities (U/MGD) in µmol TMAO reduced per MGD present in the protein (calculated as relative activities (U/mg) shown in panel A divided by relative fluorescence values in (LU/mg) in panel B). The obtained values were normalized to anaerobically expressed and aerobically purified TorA-WT set to 100%.

To analyze whether the cysteine is able to coordinate to the molybdenum ion as a ligand, we treated the TorA variant with iodoacetamide. The results in Figure 5 show that the TorA-WT activity was not influenced by the presence of iodoacetamide. Further, also the TorA-S191C variant showed no loss of activity upon iodoacetamide treatment. HPLC-ESI mass spectrometry analysis of the iodoacetamide treated TorA-S191C variant in the presence or absence of TMAO revealed a carboxamidomethylation of residue Cys191 (Figure 6). Since the carboxamidomethylation in the presence of TMAO reached almost 70%, while the enzyme activity was not influenced by the alkylation of the Cys residue, this clearly demonstrates that the cysteine is not a ligand to the molybdenum atom and that its contribution is additionally not essential for catalysis (Figure 6).

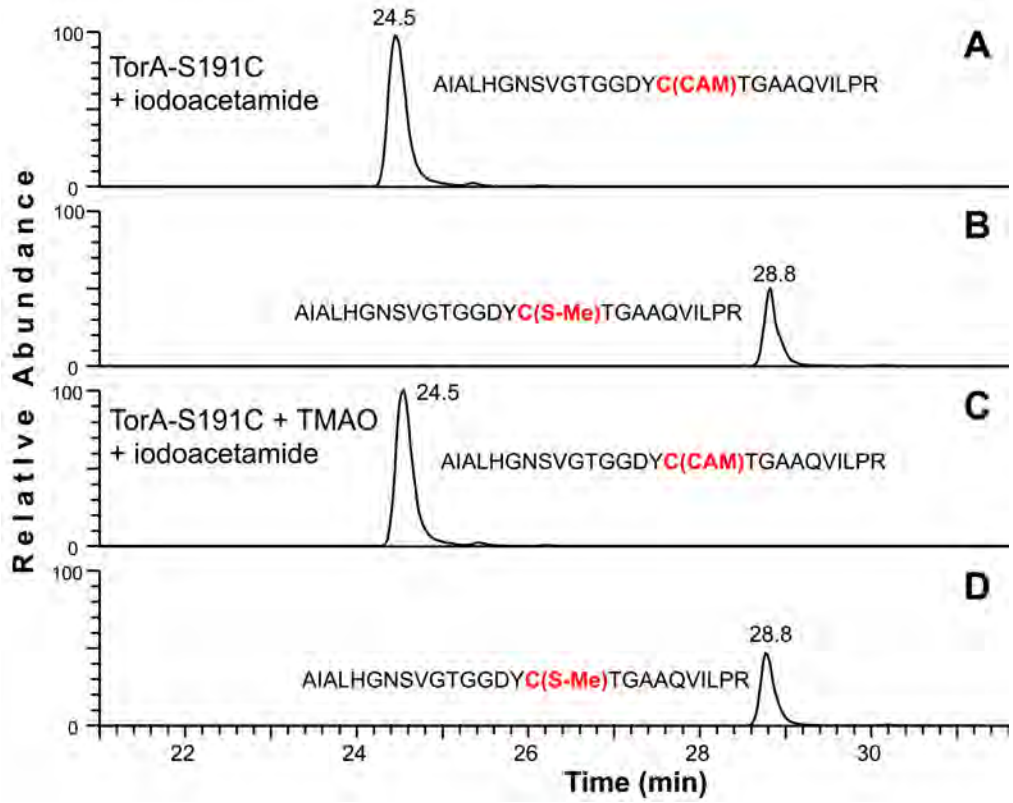

Figure 6. **Carboxamidomethylation of TorA-S191C by iodoacetamide.** HPLC-ESI-MS comparison of the tryptic peptides containing the active site cysteine of the TorA-S191C variant. Depicted are the ion traces of the triply charged molecular ions of the carboxamidomethylated (m/z = 866.776) and thiomethylated (m/z = 863.098) peptides allowing an approximate determination of their relative abundances. Thiomethylation was applied to inhibit disulfide bridge formation. The amino acid sequences of the respective peptides were verified by additional MS/MS spectra of all relevant ions (data not shown). (A) Carboxamidomethylated tryptic TorA-S191C peptide modified by iodoactamide, (B) thiomethylated analogous peptide treated with methyl methanethiosulfonate, (C) carboxamidomethylated peptide modified with iodoactamide in the presence of TMAO, (D) thiomethylated TorA-S191C treated with methyl methanethiosulfonate in the presence of TMAO.

Electrocatalytic onset potentials of TorA variants determined by direct protein-electrochemistry.

In order to determine the differences in the reduction potential derived by the presence of a sulfido ligand in the coordination sphere of TorA, we determined the onset potentials by protein-electrochemistry. After the modification of the electrode with enzyme, the electrode was immersed in the electrochemical cell and cyclic voltammetry (CV) was performed. The potential was cycled between 0 V and -0.7 V or -0.2 and -0.8 V dependent on the TorA variants and turnover currents were measured in the presence of TMAO without an additional electron acceptor. As shown in Table 1, only the anaerobically expressed TorA-WT, and the reconstituted TorA variants (recTorA), recTorA^{sulfido}Moco^{XDH}, recTorA^{sulfido}bis-MGD^{FDH}, or TorA-S191C were catalytically active by direct electrochemistry, while the other variants were inactive. Figure 7 presents the voltammograms recorded for the anaerobically expressed wild type enzyme, which was either aerobically (Figure 7A) or anaerobically purified (Figure 7B).

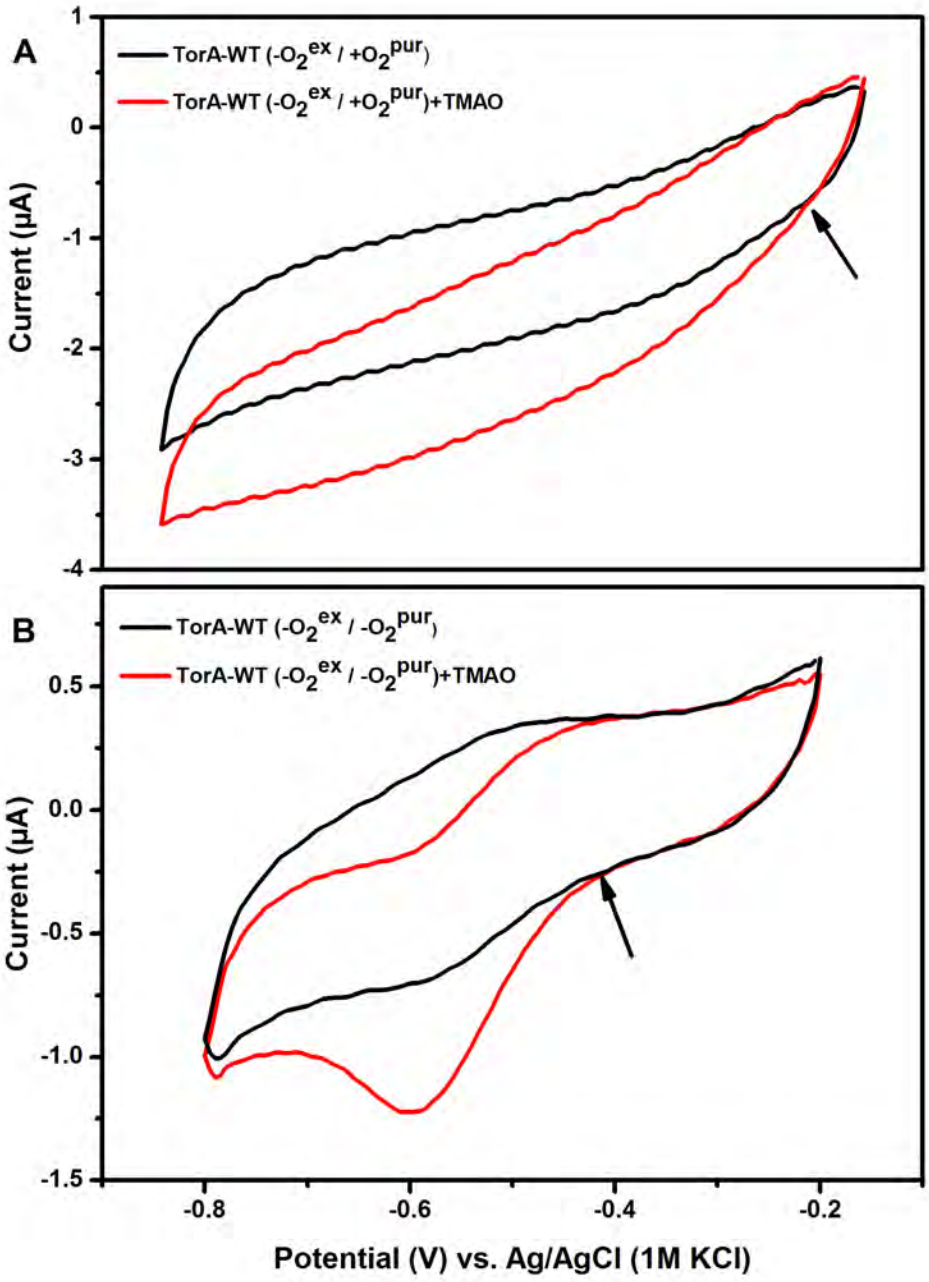

Figure 7: **Direct bioelectrocatalysis of immobilized TorA-WT with TMAO as substrate.**
(A) Cyclic voltammograms of TorA-WT anaerobically expressed and aerobically purified ($-O_2^{ex}/+O_2^{pur}$) and (B) TorA-WT anaerobically expressed and anaerobically purified ($-O_2^{ex}/-O_2^{pur}$). The black traces show the voltammogram recorded when no substrate is present and red traces measured in the presence of 3 mM TMAO in the measuring cell. The arrow points at the onset of

the catalytic current rise. Conditions: pH 6.5 10 mM phosphate buffer, 3 mM TMAO, scan rate 5 mV/s, under stirring conditions.

Both variants were also revealed to be active in solution with reduced methyl viologen as electron donor. After the addition of TMAO as substrate, the electrocatalytic reduction current emerged with a disappearance of the oxidative wave and boost of the cathodic current. The potential at which the electrocatalytic current starts to be observable, which is larger than the background current without substrate, is called onset potential (E_{onset}).[41] It is marked with a grey arrow in the graph of Figure 7 and a clear deviation can be seen in the E_{onset} between the two different TorA-WT enzymes. The E_{onset} at -0.23 V (Figure 7A) and -0.42 V (Figure 7B) indicate the starting point of the oxidation of Moco. By increase of the reduction potential, the catalytic current increased further until a limiting current was reached and was much more pronounced for the fully anaerobically produced TorA-WT (Figure 7B). The data in Table 1 show that direct electrocatalytic currents were only obtained for TorA variants which are expected to have a sulfido ligand at the Mo atom (see also supplementary Figure S1). All variants reconstituted with a Mo=O containing Moco instead did not generate an electrocatalytic response, thus, they are considered as being electrochemically inactive (Table 1). Figure S2 shows the blank reaction without enzyme while Figure S3 shows the cyclic voltammogramm (CV) for the electrocatalytically inactive TorA-WT ($+O_2^{ex}/+O_2^{pur}$) for comparison. It is obvious that substrate addition did not effect the CV wave in the blank experiments while it clearly increased the reduction wave for the catalytic reaction with active enzyme. For the anaerobically expressed and aerobically purified TorA-WT enzyme ($-O_2^{ex}/+O_2^{pur}$) the E_{onset} already starts around -0.23 V (Figure 7A). Since an E_{onset} of -0.23 V was obtained in comparison to a more negative E_{onset} of -0.42 V obtained for the anaerobically expressed and anaerobically purified TorA-WT ($-O_2^{ex}/-$

O_2^{pur}) and the variants recTorA^{sulfido}Moco^{XDH} and recTorA^{sulfido}bis-MGD^{FDH} (see also Figure S1) which were reconstituted with a sulfido-containing bis-MGD, it can be concluded that a decreased exposure of the enzyme to oxygen results in a more negative potential of the Moco. Small differences are also present for the TorA-S191C variant (see supplemental Figure S1), where the cysteine might have an additional effect on the redox potential of the Moco, even though it is not directly coordinated to the molybdenum ion (as shown in Figure 6).

Since in the solution assays with reduced benzyl viologen as electron donor, TorA activities were detected for the variants containing an oxo ligand at the active site, we additionally detected the catalytic currents after addition of methyl viologen in an amperometric experiment at -0.8 V. Figures S4 and S5 are representative examples of the current trace recorded with an enzyme loaded and an enzyme free (blank) electrode. The results in Table 1 show that with the mediator methyl viologen, bioelectrocatalysis was detected in the presence of TMAO for all enzyme variants. The results are generally comparable among each other. Conclusively, the mediator methyl viologen seems to influence the reactivity of TorA on the electrode so that activity can be measured independent on the presence of an oxo or sulfido ligand. The same might be true for the solution assays where reduced benzyl viologen was used to reduce the enzyme. Thus, in inactive TorA protein variants containing an oxo ligand, enzyme activity might have been observed due to an artificial activating effect of methyl viologen in the assay.

EPR characterization of aerobically and anaerobically expressed TorA.

For the first time, TorA was characterized by EPR spectroscopy. Here, our goal was to differentiate the sulfido-containing bis-MGD cofactor from the oxo-containing bis-MGD form. Consistent with the activity data (Figure 1), differences in the Mo(V) signals were observed for

samples expressed under anaerobic versus aerobic conditions under selected redox conditions (Figure 8, see also Figure S6 and Table S1).

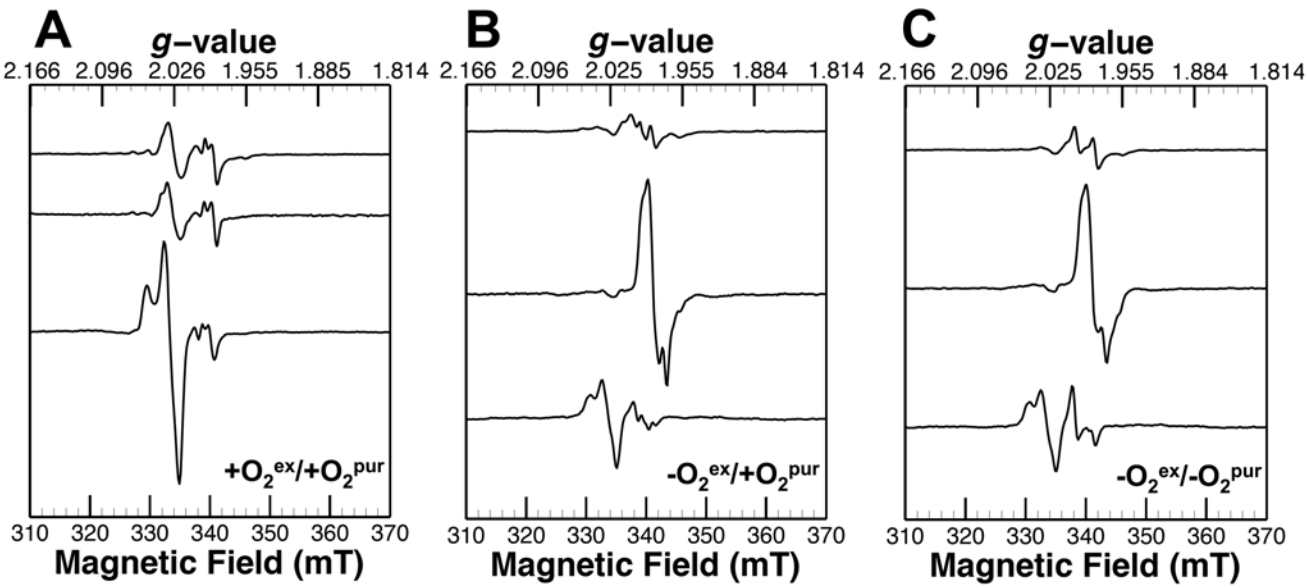

Figure 8: **X-Band Electron Paramagnetic Resonance Redox Profile of TorA^{WT} Samples.**
(A) depicts aerobically expressed and purified TorA ($+O_2^{ex}/+O_2^{pur}$), (B) depicts TorA expressed anaerobically but purified aerobically ($-O_2^{ex}/+O_2^{pur}$), while (C) depicts TorA expressed and purified anaerobically ($-O_2^{ex}/-O_2^{pur}$). Protein depicted in (C) originated from the same batch of anaerobically expressed enzyme. For each panel, the top spectrum depicts the sample as-isolated, middle spectrum depicts treatment with 10 mM sodium dithionite, while the bottom spectrum depicts treatment with 10 mM $Na_3Fe(CN)_6$. Spectra were obtained at 80 K at 3.93 mW microwave power, 5 G modulation amplitude and at a 100 kHz modulation frequency. Spectra have been scaled to represent a concentration of TorA of 100 μM.

As-isolated samples possessed multiple overlapping species present (Figure 8, top traces; and Figure S6), but a more simplified spectrum was observed for the TorA-WT ($-O_2^{ex}/+O_2^{pur}$) sample (Figure 8A, top trace). Similar to DMSO reductase from *R. capsulatus*[42-44] and arsenite oxidase from *A. faecalis*[45], the percent of integrated signal relative to the Mo concentration in the as-isolated state was low (Table S1), which represented only 3 - 4% of the overall quantity of Mo

present. Nevertheless, TorA-WT ($-O_2^{ex}/-O_2^{pur}$) exhibited largely rhombic signal with *g*-values of 1.987, 1.965, and 1.941 (g_{av} = 1.964, g_1-g_3 = 0.046) (Figure S7). Other spectral components detected among as-isolated TorA-WT spectra included two axial signals at 330-333 mT and at 339-342 mT (Figure 8A top trace, see also Figure S6 top trace); the latter signal could also be observed in the TorA-WT ($+O_2^{ex}/+O_2^{pur}$) sample (Figure 8B top trace, see also Figure S6 middle trace). However, these signals were largely absent in the TorA-WT ($-O_2^{ex}/-O_2^{pur}$) spectrum, suggesting that the rhombic signal is associated with a sulfurated bis-MGD species (Figure 8B and C, top traces; Figure S6, top and middle traces; Figure S7).

Notable differences in TorA-WT Mo(V) signals were observed upon treatment with redox agents. Treatment of TorA-WT samples with either TMA or TMAO resulted in negligible spectral changes relative to as-isolated spectra (data not shown). Interestingly, sodium dithionite reduction of anaerobically expressed TorA-WT ($-O_2^{ex}/+O_2^{pur}$, $-O_2^{ex}/-O_2^{pur}$) samples resulted in generation of a new signal at higher field (lowered g_{av}) with a spin concentration at least doubled relative to as-isolated spectra, respectively. The resultant signal was similar to the low-*g* type species reported for DMSO reductase (Figure 8B + C, middle traces).[42, 43] By comparison, very minor changes were observed upon exposure to dithionite in the aerobic enzyme (Figure 8A, top and middle traces). Oxidative treatment of TorA-WT with ferricyanide resulted in generation of an axial signal at 330-336 mT, however, its generation appeared to be independent of sample anaerobicity and it predominated the TorA-WT ($+O_2^{ex}/+O_2^{pur}$) spectrum (Figure 8A-C, bottom spectra). The remaining signal in ferricyanide-oxidized samples were largely similar to as-isolated signals, with a similar rhombic signal observed in TorA-WT ($-O_2^{ex}/-O_2^{pur}$). Collectively, these results suggest that the rhombic signal in the as-isolated TorA-WT ($-O_2^{ex}/-O_2^{pur}$) spectrum is likely associated as a sulfurated bis-MGD species.

EPR characterization of in vitro-reconstituted TorA.

EPR spectral characterization of $^{sulfido}Moco^{XDH}$ and ^{sulfido}bis-MGD^{FDH} was performed to compare Mo(V) species associated with bis-MGD sources with a more clearly defined sulfido ligand. Similar to the TorA-WT ($-O_2^{ex}/-O_2^{pur}$) as-isolated spectrum, a rhombic signal was observed in as-obtained recTorA $^{sulfido}Moco^{XDH}$ and recTorA ^{sulfido}bis-MGD^{FDH} (Figure 9A).

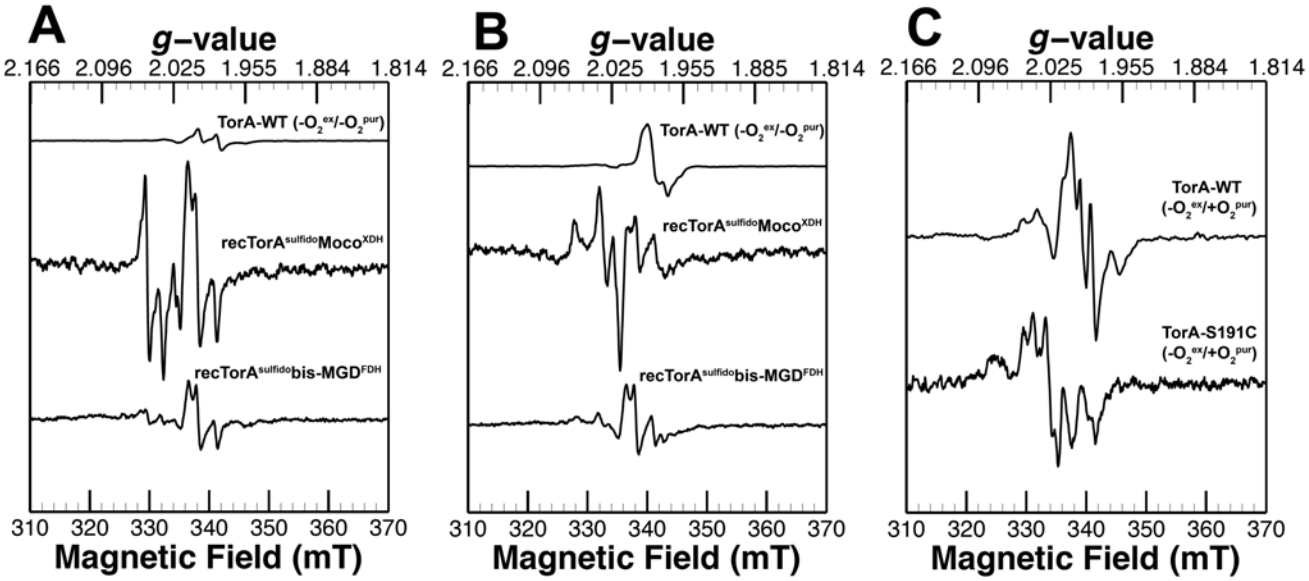

Figure 9**: X-Band EPR Characterization of TorA Variants.**

(A) and (B) depict as-obtained and dithionite-reduced (10 mM) TorA-WT (top trace), recTorA$^{sulfido}Moco^{XDH}$ (middle trace) and recTorA$^{sulfido}Moco^{FDH}$ (bottom trace) samples, respectively. (C) depicts TorA-WT (top trace) and TorA-S191C (bottom trace) that were expressed anaerobically and purified aerobically ($-O_2^{ex}/+O_2^{pur}$). The TorA-WT data of (A) and (B) represent the TorA-WT data depicted in Figure 8C, and for (C) represents TorA-WT data depicted in Figure 8B, respectively. Spectra in all panels have been scaled to represent a molybdenum concentration of TorA of 100 μM. Spectra were obtained at 80 K at 3.93 mW microwave power, 5 G modulation amplitude and at a 100 kHz modulation frequency.

Simulation of the main signal in the as-obtained recTorA ^{sulfido}bis-MGD^{FDH} spectrum yielded a component with principal *g*-values of 1.997, 1.986, and 1.967 (g_{av} = 1.983, g_1-g_3 = 0.030) (Figure S9). This signal is similar to the as-isolated TorA-WT (-O_2^{ex}/-O_2^{pur}) sample, which had an increased g_{av} and a decreased linewidth. By comparison, an additional axial signal at 328-336 mT was observed in recTorA ^{sulfido}Moco^{XDH} and recTorA ^{sulfido}bis-MGD^{FDH} as a major and minor species, respectively (Figure 9A, middle and bottom traces). However, the similarity of the simulated rhombic signal here to TorA-WT suggests that it is a common element associated with sulfurated bis-MGD.

Treatment of recTorA ^{sulfido}Moco^{XDH} and recTorA ^{sulfido}bis-MGD^{FDH} with sodium dithionite resulted in distinct generation of Mo(V) signals relative to the TorA-WT (Figure 9B). While generation of the signal at 343-347 mT in TorA-WT (-O_2^{ex}/-O_2^{pur}) could be detected in recTorA samples, it was by comparison a minor component (Figure 9B, top and bottom traces). Conservative changes accompanied dithionite addition to recTorA^{sulfido}bis-MGD^{FDH}, yielding a signal similar to the as-obtained spectrum (Figure 9A-B, bottom traces). By comparison, dithionite reduction of recTorA^{sulfido}Moco^{XDH} was more heterogeneous, particularly in the introduction of a low field rhombic signal distinct from that in the as-obtained state (Figure 9B, middle trace). This signal is similar to a signal reported in *R. capsulatus* DMSO reductase assigned to represent a sulfur-centered pterin radical.[44, 46] Thus, these spectral results suggest that the different response to dithionite between recTorA^{sulfido}bis-MGD^{FDH} and TorA-WT (-O_2^{ex}/-O_2^{pur}) imply an altered homogeneity of the TorA bis-MGD, with the as-obtained signal in recTorA^{sulfido}bis-MGD^{FDH} associated to represent a sulfurated bis-MGD species.

EPR characterization of the TorA-S191C variant.

The TorA-S191C variant that was expressed anaerobically and purified aerobically ($-O_2^{ex}/+O_2^{pur}$) was characterized by EPR spectroscopy to compare the electronic effects of the serine to cysteine exchange at the bis-MGD cofactor. Figure 9C (bottom trace) depicts TorA-S191C under as-isolated conditions. Relative to TorA-WT, the whole spectrum is shifted toward lower field for TorA-S191C, resulting in an increased g_{av}. The spin quantification of the as-isolated TorA-S191C Mo(V) signal was decreased relative to that observed in TorA-WT (Figure 9C, and Table S1). However, the signal appeared to have structure, and qualitatively appeared similar to the *R. sphaeroides* DorA-S147C variant[47], with similar overlapping features. The spectrum represents at least two discrete species that are distinct from the *R. sphaeroides* DMSO reductase that have an overall higher g_{av} (Figure 9C).[47] Following the general trend regarding the number of sulfur atoms that is reported to affect the Mo(V) g_{av}[48-50], it appears that the serine substitution for cysteine resulted in an increased g_{av}.

DISCUSSION

The reduction of TMAO to TMA by TorA involves two-electron reduction chemistry coupled to the transfer of an oxygen atom and two protons to form water.[12] The active site of the oxidized Mo(VI) enzyme has been suggested previously to be six-coordinated with two pyranopterin dithiolene ligands providing four sulfur donors to the metal, one terminal oxo ligand and a coordinating serine residue.[20] In this report, we present clear evidence that a sulfido ligand is present in catalytically active *E. coli* TorA instead of the oxo ligand (Figure 10A).

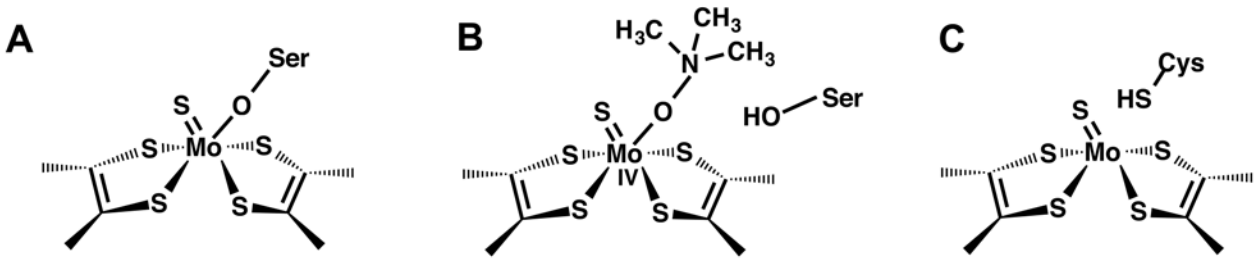

Figure 10: **Proposed active site structures of TorA.**

(A) Proposed active site structure of TorA containing two dithiolene ligands, one sulfido group, and one oxygen group from serine in the oxidized Mo(VI) state. (B) The substrate binds to the reduced Mo(IV) and displaces the serine ligand. (C) In the TorA-S191C variant, the cysteine is not a ligand to the molybdenum atom.

We started our investigations based on the fact that in *E. coli,* the TorA protein was shown to be present both under aerobic and anaerobic conditions.[21] However, the aerobically expressed protein proved to be significantly less active with an activity of approximately 5% in comparison to the anaerobically expressed enzyme.[8] By different corroborative methods, we provide evidence that the aerobically expressed enzyme contains the oxo ligand at the active site, while the anaerobically expressed enzyme contains a sulfido ligand (Figure 10A). Thus, we conclude from our data that the bis-MGD cofactor is damaged during aerobic purification of the enzyme, shown by a reduced bis-MGD content of the enzyme, 30% reduced enzyme activities and a more heterogeneous EPR Mo(V) spectrum. Additionally, the onset potential in the direct electrochemistry of the enzyme on the electrode was shown to be more positive in the aerobically purified enzyme, also revealing a modified, likely oxidatively damaged form of the bis-MGD cofactor. Therefore, we conclude that during aerobic expression in the cell, the bis-MGD cofactor is oxidatively damaged resulting further in the loss of the sulfido ligand. The enzyme directly reconstituted with sulfido-containing bis-MGD, instead, showed a high activity and a relatively more simplified EPR spectrum. This interpretation is consistent with a previous study on the

characterization of *E. coli* TorA active site by X-ray absorption spectroscopy. In this study, the inactive as-isolated enzyme was used, revealing that one dithiolene group of the bis-MGD was dissociated from the molybdenum atom which consequently contributed to the inactivity of the enzyme.[20] An active form of the enzyme was only obtained after redox cycling with dithionite. The X-ray absorption spectroscopy data obtained for the redox-cycled enzyme were interpreted to contain a molybdenum coordination environment with four dithiolene-based sulfur atoms, one double bonded oxygen ligand and one serine-based oxygen ligand from the protein backbone. In contrast to these data, the interpretation of the crystal structure data from *S. massilia* TMAO reductase[11] (*E. coli* and *S. massilia* TMAO reductases share 49% sequence identity and 67% sequence similarities) has suggested a molybdenum coordination sphere with two dithiolene sulfur ligands and three oxygen ligands (one from serine). The existing data overall imply that in previous studies different forms of TMAO reductase were obtained, due to oxidative damage of the cofactor in the enzyme or partial photoreduction during data collection. Similar observations have been made for DMSO reductase from *R. capsulatus* and *R. sphaeroides*, where three different crystal structures were derived showing different Mo species in the active site.[17, 51-53]

EPR characterizations of TorA in this study also showed that the active site is heterogeneous with respect to identifiable Mo(V) species present. Similar behavior has been reported for DMSO reductase[42-44] in the quantity and type of species present. Thus, TMAO reductase harbors several paramagnetic species that are observable by EPR spectroscopy, which are dependent on the method of enzyme handling and show a distinct behavior to different redox treatments. A more simplified Mo(V) EPR spectrum could be identified in apo-TorA reconstituted with the bis-MGD cofactor extracted from *R. capsulatus* FDH. Here, our data provide first-time evidence that the bis-MGD cofactor can be extracted from molybdoenzymes,

and that this cofactor remains intact for at least 90 minutes outside of the protein environment. The extracted cofactor was inserted into apo-TorA, which gained comparable activity but higher homogeneity in comparison to the enzyme purified under anaerobic conditions from *E. coli* cells, thus, the cofactor extraction and insertion procedures preserves an intact bis-MGD cofactor that is inserted with a proper coordinating environment into apo-TorA. Further, the sulfido-ligand seems to remain coordinated at the extracted bis-MGD cofactor, as evidenced by the EPR spectra.

Our studies by direct electrochemistry proved that the enzyme showed substrate-dependent electrocatalytic activity when the sulfido ligand was present at the active site. Further, a fully saturated ligand sphere with the sulfido ligand resulted in the shift of the apparent onset potential to the more negative region, resulting in the most negative onset potentials for recTorA^{sulfido}Moco^{XDH} and recTorA^{sulfido}bis-MGD^{FDH} reconstituted enzymes. Likely, the enzyme expressed under anaerobic conditions, but purified under aerobic conditions contained a partially oxidative damaged cofactor, which resulted in a more positive onset potential. The fact that onset potentials in the direct electrochemistry were only obtained when a sulfido ligand was present at the molybdenum site and not an oxo ligand may reflect that the sulfido-containing bis-MGD adopts a different conformation in the enzyme, resulting in a form that is able to directly communicate with the electrode. Furthermore, the sulfur ligand modulates probably the redox potentials of the Mo ion into the range required for TMAO reduction. Since the cofactor is deeply buried in the enzyme, the cofactor has to move more towards the surface of the substrate-binding pocket. This model is consistent with a previous investigation by Rothery, Kirk, Weiner and coworkers, who showed a conformational flexibility of the bis-MGD cofactor in dependence on its reduction state.[54] When mediated electrochemistry was performed with methyl viologen as

artificial redox mediator, electrocatalysis was obtained for all enzymes, and was independent of the presence or absence of the sulfido ligand in the enzyme. Thus, the artificial electron mediators methyl viologen or benzyl viologen used in the electrochemistry or solution assays, respectively, seem to modulate the enzyme in a manner that enzymatic activity can be obtained. This might be based on an interaction of the mediators with the cofactor, resulting in a similar conformation as the sulfido-containing bis-MGD, consequently enabling the communication with the electrode.

The replacement of the active site serine 191 by a cysteine resulted in a catalytically active enzyme and alkylation studies revealed that the cysteine is not a ligand to the Mo atom. A similar observation has been recently proposed for *R. sphaeroides* DMSO reductase, a homologous enzyme to TMAO reductase coordinating the bis-MGD cofactor with four dithiolene sulfurs, one oxo ligand and a serine ligand in the oxidized state.[55] Recent studies by DFT calculations of the available crystal structure data and extended X-ray absorption fine structure (EXAFS) studies have suggested that the Ser147 in DMSO reductase has more flexibility than previously suggested and that it might be able to dissociate from the molybdenum atom.[56] Characterization of the Mo(V) oxidation state of TorA-S191C by EPR spectroscopy showed relative to TorA-WT a shifted spectrum corresponding to a higher g_{av}, suggesting that the ligand imposes electronic differences on the bis-MGD and likewise support ligand-molybdenum atom dissociation.

Overall, we suggest a novel substrate-binding mode of TMAO at the molybdenum site (Figure 10). With a sulfido ligand in place of the oxo ligand, the Mo(IV/V/VI) is tuned to the appropriate redox range for TMAO reduction. The substrate can not bind at the position of the sulfido ligand, otherwise the sulfido ligand is lost after one substrate turnover, resulting in an inactive enzyme. Therefore, we suggest that the substrate TMAO binds in place of the serine ligand at the active site (Figure 10B). This mechanism would be similar to the suggested mechanism of *Ralstonia*

eutropha nitrate reductase and the mechanism suggested for nitrate reduction by *R. capsulatus* FDH.[15, 18] The displacement of the serine ligand is supported by the data obtained for the TorA-S191C variant (Figure 10C), for which a 100% alkylation of the cysteine ligand was shown after iodoacetamide treatment, while the protein retained its activity. Thus, at least in the TorA-S191C variant, the cysteine is not a ligand to the molybdenum atom and the substrate is proposed to bind to the free coordination site at the molybdenum atom.

Conclusively, it has to be considered also for other enzymes of the DMSO reductase family that a sulfido ligand might be present at the molybdenum atom, since TMAO reductase represents the third enzyme in addition to nitrate reductase and FDH for which a sulfido ligand has been identified.[15, 16, 18] Anaerobic expression and purification might be obligatory for conserving the intact Mo coordination environment.

AUTHOR INFORMATION

Corresponding Author

*To whom correspondence should be addressed: Silke Leimkühler, Institute of Biochemistry and Biology, Department of Molecular Enzymology, University of Potsdam, Karl-Liebknecht-Str. 24-25, 14476 Potsdam, Germany, Telephone: +49-331-977-5603; Fax: +49-331 977-5128; E-mail: sleim@uni-potsdam.de

FUNDING

This work was supported by the cluster of excellence 314 “Unicat” (to C.T., U.W. and S.L.), funded by the DFG, in addition to grant LE1171/6-2 (to S.L).

NOTES:

The authors declare they have no conflicts of interest with the contents of this article.

ACKNOWLEDGEMENT

We thank Angelika Lehmann (Potsdam) for protein purification and technical assistance.

SUPPORTING INFORMATION AVAILABLE

Supplementary Table S1 and Figures S1 to S9.

Table S1: TorA sample protein, Mo, and spin concentrations used in EPR spectroscopy.

Figure S1: Direct bioelectrocatalysis of active TorA variants with TMAO as substrate.

Figure S2: Cyclic voltammogram of the blank electrode (no enzyme immobilized) in the presence and absence of TMAO.

Figure S3: Direct bioelectrocatalysis of immobilized aerobically expressed and purified TorA-WT with TMAO as substrate.

Figure S4: Amperometric curves for mediated bioelectrocatalysis.

Figure S5: Amperometric curves for the blank electrode.

Figure S6: Zoomed-in view of as-isolated TorA-WT EPR spectra.

Figure S7: EPR spectral simulation of TorA-WT ($-O_2^{ex}$/$-O_2^{pur}$) in the as-isolated state.

Figure S8: EPR spectral simulation of recTorA^{sulfido}bis-MGD^{FDH} in the as-obtained state.

REFERENCES

[1] Stewart, V. (1988) Nitrate respiration in relation to facultative metabolism in enterobacteria, *Microbiol. Rev. 52*, 190-232.

[2] Unden, G., Becker, S., Bongaerts, J., Holighaus, G., Schirawski, J., and Six, S. (1995) O_2-sensing and O_2-dependent gene regulation in facultatively anaerobic bacteria, *Arch Microbiol 164*, 81-90.

[3] McCrindle, S. L., Kappler, U., and McEwan, A. G. (2005) Microbial dimethylsulfoxide and trimethylamine-*N*-oxide respiration, *Adv Microb Physiol 50*, 147-198.

[4] Gon, S., Giudici-Orticoni, M. T., Mejean, V., and Iobbi-Nivol, C. (2001) Electron transfer and binding of the c-type cytochrome TorC to the trimethylamine N-oxide reductase in *Escherichia coli*, *J Biol Chem 276*, 11545-11551.

[5] Mejean, V., Iobbi-Nivol, C., Lepelletier, M., Giordano, G., Chippaux, M., and Pascal, M. C. (1994) TMAO anaerobic respiration in *Escherichia coli*: involvement of the tor operon, *Mol Microbiol 11*, 1169-1179.

[6] Iobbi-Nivol, C., Pommier, J., Simala-Grant, J., Mejean, V., and Giordano, G. (1996) High substrate specificity and induction characteristics of trimethylamine-*N*-oxide reductase of *Escherichia coli*, *Biochim Biophys Acta 1294*, 77-82.

[7] Simon, G., Mejean, V., Jourlin, C., Chippaux, M., and Pascal, M. C. (1994) The *torR* gene of *Escherichia coli* encodes a response regulator protein involved in the expression of the trimethylamine *N*-oxide reductase genes, *J Bacteriol 176*, 5601-5606.

[8] Bühning, M., Valleriani, A., and Leimkühler, S. (2017) The Role of SufS Is Restricted to Fe-S Cluster Biosynthesis in *Escherichia coli*, *Biochemistry 56*, 1987-2000.

[9] Wissenbach, U., Ternes, D., and Unden, G. (1992) An *Escherichia coli* mutant containing only demethylmenaquinone, but no menaquinone: effects on fumarate, dimethylsulfoxide, trimethylamine *N*-oxide and nitrate respiration, *Arch Microbiol 158*, 68-73.

[10] Wissenbach, U., Kroger, A., and Unden, G. (1990) The specific functions of menaquinone and demethylmenaquinone in anaerobic respiration with fumarate, dimethylsulfoxide, trimethylamine N-oxide and nitrate by *Escherichia coli*, *Arch Microbiol 154*, 60-66.

[11] Czjzek, M., Dos Santos, J. P., Pommier, J., Giordano, G., Mejean, V., and Haser, R. (1998) Crystal structure of oxidized trimethylamine N-oxide reductase from *Shewanella massilia* at 2.5 A resolution, *Journal of molecular biology 284*, 435-447.

[12] Hille, R., Hall, J., and Basu, P. (2014) The mononuclear molybdenum enzymes, *Chemical reviews 114*, 3963-4038.

[13] Hille, R. (1996) The mononuclear molybdenum enzymes, *Chemical Rev 96*, 2757-2816.

[14] Leimkühler, S., and Iobbi-Nivol, C. (2016) Bacterial molybdoenzymes: old enzymes for new purposes, *FEMS microbiology reviews 40*, 1-18.

[15] Coelho, C., Gonzalez, P. J., Moura, J. G., Moura, I., Trincao, J., and Joao Romao, M. (2011) The crystal structure of *Cupriavidus necator* nitrate reductase in oxidized and partially reduced states, *Journal of molecular biology 408*, 932-948.

[16] Raaijmakers, H. C., and Romao, M. J. (2006) Formate-reduced *E. coli* formate dehydrogenase H: The reinterpretation of the crystal structure suggests a new reaction mechanism, *J Biol Inorg Chem 11*, 849-854.

[17] Schindelin, H., Kisker, C., Hilton, J., Rajagopalan, K. V., and Rees, D. C. (1996) Crystal structure of DMSO reductase: redox-linked changes in molybdopterin coordination, *Science 272*, 1615-1621.

[18] Hartmann, T., Schrapers, P., Utesch, T., Nimtz, M., Rippers, Y., Dau, H., Mroginski, M. A., Haumann, M., and Leimkühler, S. (2016) The Molybdenum Active Site of Formate

Dehydrogenase Is Capable of Catalyzing C-H Bond Cleavage and Oxygen Atom Transfer Reactions, *Biochemistry 55*, 2381-2389.

[19] Warelow, T. P., Pushie, M. J., Cotelesage, J. J. H., Santini, J. M., and George, G. N. (2017) The active site structure and catalytic mechanism of arsenite oxidase, *Sci Rep 7*, 1757.

[20] Zhang, L., Nelson, K. J., Rajagopalan, K. V., and George, G. N. (2008) Structure of the molybdenum site of *Escherichia coli* trimethylamine N-oxide reductase, *Inorg Chem 47*, 1074-1078.

[21] Ansaldi, M., Theraulaz, L., Baraquet, C., Panis, G., and Mejean, V. (2007) Aerobic TMAO respiration in *Escherichia coli*, *Mol Microbiol 66*, 484-494.

[22] Genest, O., Ilbert, M., Mejean, V., and Iobbi-Nivol, C. (2005) TorD, an essential chaperone for TorA molybdoenzyme maturation at high temperature, *J Biol Chem 280*, 15644-15648.

[23] Temple, C. A., and Rajagopalan, K. V. (2000) Mechanism of assembly of the Bis(Molybdopterin guanine Dinucleotide)Molybdenum cofactor in *Rhodobacter sphaeroides* dimethyl sulfoxide reductase, *J Biol Chem 275*, 40202-40210.

[24] Neumann, M., Schulte, M., Jünemann, N., Stöcklein, W., and Leimkühler, S. (2006) *Rhodobacter capsulatus* XdhC is involved in molybdenum cofactor binding and insertion into xanthine dehydrogenase, *J Biol Chem 281*, 15701-15708.

[25] Leimkühler, S., Hodson, R., George, G. N., and Rajagopalan, K. V. (2003) Recombinant *Rhodobacter capsulatus* xanthine dehydrogenase, a useful model system for the characterization of protein variants leading to xanthinuria I in humans, *J Biol Chem 278*, 20802-20811.

[26] Hartmann, T., and Leimkühler, S. (2013) The oxygen-tolerant and NAD-dependent formate dehydrogenase from *Rhodobacter capsulatus* is able to catalyze the reduction of CO_2 to formate, *The FEBS journal 280*, 6083-6096.

[27] Neumann, M., Stöcklein, W., and Leimkühler, S. (2007) Transfer of the Molybdenum Cofactor Synthesized by *Rhodobacter capsulatus* MoeA to XdhC and MobA, *J Biol Chem 282*, 28493-28500.

[28] Johnson, J. L., Rajagopalan, K. V., and Meyer, O. (1990) Isolation and characterization of a second molybdopterin dinucleotide: molybdopterin cytosine dinucleotide, *Arch. Biochem. Biophys. 283*, 542-545.

[29] Johnson, K. E., and Rajagopalan, K. V. (2001) An active site tyrosine influences the ability of the dimethyl sulfoxide reductase family of molybdopterin enzymes to reduce S-oxides, *J Biol Chem 276*, 13178-13185.

[30] Niks, D., Duvvuru, J., Escalona, M., and Hille, R. (2016) Spectroscopic and Kinetic Properties of the Molybdenum-containing, NAD^+-dependent Formate Dehydrogenase from *Ralstonia eutropha*, *J Biol Chem 291*, 1162-1174.

[31] Stoll, S., and Schweiger, A. (2006) EasySpin, a comprehensive software package for spectral simulation and analysis in EPR, *Journal of magnetic resonance 178*, 42-55.

[32] Hänzelmann, P., Dobbek, H., Gremer, L., Huber, R., and Meyer, O. (2000) The effect of intracellular molybdenum in *Hydrogenophaga pseudoflava* on the crystallographic structure of the seleno-molybdo-iron-sulfur flavoenzyme carbon monoxide dehydrogenase, *J Mol Biol 301*, 1221-1235.

[33] Reschke, S., Sigfridsson, K. G., Kaufmann, P., Leidel, N., Horn, S., Gast, K., Schulzke, C., Haumann, M., and Leimkühler, S. (2013) Identification of a Bis-molybdopterin

Intermediate in Molybdenum Cofactor Biosynthesis in *Escherichia coli*, *J Biol Chem 288*, 29736-29745.

[34] Genest, O., Neumann, M., Seduk, F., Stocklein, W., Mejean, V., Leimkühler, S., and Iobbi-Nivol, C. (2008) Dedicated metallochaperone connects apoenzyme and molybdenum cofactor biosynthesis components, *J Biol Chem 283*, 21433-21440.

[35] Ilbert, M., Mejean, V., Giudici-Orticoni, M. T., Samama, J. P., and Iobbi-Nivol, C. (2003) Involvement of a mate chaperone (TorD) in the maturation pathway of molybdoenzyme TorA, *J Biol Chem 278*, 28787-28792.

[36] Leimkühler, S., Stockert, A. L., Igarashi, K., Nishino, T., and Hille, R. (2004) The role of active site glutamate residues in catalysis of *Rhodobacter capsulatus* xanthine dehydrogenase, *J Biol Chem 279*, 40437-40444.

[37] Reschke, S., Mebs, S., Sigfridsson-Clauss, K. G., Kositzki, R., Leimkühler, S., and Haumann, M. (2017) Protonation and Sulfido versus Oxo Ligation Changes at the Molybdenum Cofactor in Xanthine Dehydrogenase (XDH) Variants Studied by X-ray Absorption Spectroscopy, *Inorg Chem 56*, 2165-2176.

[38] Wahl, R. C., and Rajagopalan, K. V. (1982) Evidence for the inorganic nature of the cyanolyzable sulfur of molybdenum hydroxylases, *J Biol Chem 257*, 1354-1359.

[39] Neumann, M., Stöcklein, W., Walburger, A., Magalon, A., and Leimkühler, S. (2007) Identification of a *Rhodobacter capsulatus* L-cysteine desulfurase that sulfurates the molybdenum cofactor when bound to XdhC and before its insertion into xanthine dehydrogenase, *Biochemistry 46*, 9586-9595.

[40] Schrapers, P., Hartmann, T., Kositzki, R., Dau, H., Reschke, S., Schulzke, C., Leimkühler, S., and Haumann, M. (2015) Sulfido and cysteine ligation changes at the molybdenum

cofactor during substrate conversion by formate dehydrogenase (FDH) from *Rhodobacter capsulatus*, *Inorg Chem 54*, 3260-3271.

[41] Adamson, H., Simonov, A. N., Kierzek, M., Rothery, R. A., Weiner, J. H., Bond, A. M., and Parkin, A. (2015) Electrochemical evidence that pyranopterin redox chemistry controls the catalysis of YedY, a mononuclear Mo enzyme, *Proc Natl Acad Sci U S A 112*, 14506-14511.

[42] Bennett, B., Benson, N., McEwan, A. G., and Bray, R. C. (1994) Multiple states of the molybdenum centre of dimethylsulphoxide reductase from *Rhodobacter capsulatus* revealed by EPR spectroscopy, *Eur J Biochem 225*, 321-331.

[43] Bennett, B., Benson, N., McEwan, A. G., and Bray, R. C. (1994) E.p.r. characterisation of the molybdenum centre of *Rhodobacter capsulatus* dimethylsulphoxide reductase: new signals on reduction with Na2S2O4, *Biochem Soc Trans 22*, 285S.

[44] Lane, I. (2004) Electron Paramagnetic Resonance Studies of *Rhodobacter capsulatus* Dimethysulfoxide Reductase, Model Mo(V) and W(V) Complexes and Metallotolyporphyrins, In *Department of Chemistry*, University of Queensland, School of Molecular and Microbial Sciences.

[45] Duval, S., Santini, J. M., Lemaire, D., Chaspoul, F., Russell, M. J., Grimaldi, S., Nitschke, W., and Schoepp-Cothenet, B. (2016) The H-bond network surrounding the pyranopterins modulates redox cooperativity in the molybdenum-bisPGD cofactor in arsenite oxidase, *Biochim Biophys Acta 1857*, 1353-1362.

[46] Hanson, G. R., and Lane, I. (2010) Applications of High-Resolution EPR to Metalloenzymes In *Metals in Biology* (Hanson, G., and Berliner, L., Eds.), pp 169-199, Springer Science + Business Media, New York.

[47] George, G. N., Hilton, J., Temple, C., Prince, R. C., and Rajagopalan, K. V. (1999) Structure of the molybdenum site of dimethyl sulfoxide reductase, *J. Am. Chem. Soc. 121*, 1256-1266.

[48] Cleland, W. E., Barnhart, K. M., Yamanouchi, K., Collison, D., Mabbs, F. E., Ortega, R. B., and Enemark, J. H. (1987) Syntheses, Structures, and Spectroscopic Properties of 6-Coordinate Mononuclear Oxo-Molybdenum(V) Complexes Stabilized by the Hydrotris(3,5-Dimethyl-1-Pyrazolyl)Borate Ligand, *Inorg Chem 26*, 1017-1025.

[49] Young, C. G., Enemark, J. H., Collison, D., and Mabbs, F. E. (1987) The 1st Mononuclear Molybdenum(V) Complex with a Terminal Sulfido Ligand - [Hb(Me2c3n2h)3]Moscl2, *Inorg Chem 26*, 2925-2927.

[50] Gladyshev, V. N., Khangulov, S. V., Axley, M. J., and Stadtman, T. C. (1994) Coordination of selenium to molybdenum in formate dehydrogenase H from *Escherichia coli*, *Proc. Natl. Acad. Sci. U. S. A. 91*, 7708-7711.

[51] McAlpine, A. S., McEwan, A. G., and Bailey, S. (1998) The high resolution crystal structure of DMSO reductase in complex with DMSO, *J Mol Biol 275*, 613-623.

[52] Schneider, F., Löwe, J., Huber, R., Schindelin, H., Kisker, C., and Knäblein, J. (1996) Crystal structure of dimethyl sulfoxide reducatase from *Rhodobacter capsulatus* at 1.88 Å resolution, *J. Mol. Biol. 263*, 53-69.

[53] Li, H. L., Temple, C., Rajagopalan, K. V., and Schindelin, H. (2000) The 1.3 Å Crystal Structure of Rhodobacter sphaeroides Dimethyl Sulfoxide Reductase Reveals Two Distinct Molybdenum Coordination Environments, *J Am Chem Soc 122*, 7673-7680.

[54] Rothery, R. A., Stein, B., Solomonson, M., Kirk, M. L., and Weiner, J. H. (2012) Pyranopterin conformation defines the function of molybdenum and tungsten enzymes, *Proc Natl Acad Sci U S A 109*, 14773-14778.

[55] Pushie, M. J., Cotelesage, J. J., Lyashenko, G., Hille, R., and George, G. N. (2013) X-ray absorption spectroscopy of a quantitatively Mo(V) dimethyl sulfoxide reductase species, *Inorg Chem 52*, 2830-2837.

[56] Dong, G., and Ryde, U. (2017) Effect of the protein ligand in DMSO reductase studied by computational methods, *J Inorg Biochem 171*, 45-51.

Table 1: List of TorA-variants investigated for direct (DET) and mediated (MET) electrocatalysis after immobilization and the values for E_{onset}.

TorA variants	**DET[a] E_{onset}/ V**	**MET[b] I/µA**
TorA-WT ($-O_2^{ex}/-O_2^{pur}$)	**-0.42 ± 0.03**	**83.16 ± 3.50**
TorA-WT ($-O_2^{ex}/+O_2^{pur}$)	**-0.23 ± 0.01**	**63.16 ± 5.26**
TorA-WT ($+O_2^{ex}/+O_2^{pur}$)	**-[c]**	**47.18 ± 7.90**
recTorA^{sulfido}Moco^{XDH}	**-0.45 ± 0.03**	**55.20 ± 5.86**
recTorA^{oxo}Moco$^{XDH+KCN}$	**-**	**53.28 ± 2.73**
recTorA^{oxo}Moco$^{XDH/\Delta XdhC}$	**-**	**17.52 ± 1.47**
recTorA^{sulfido}Moco$^{XDH/KCN+sulfide}$	**-**	**25.14 ± 2.80**
recTorA^{sulfido}bis-MGD^{FDH}	**-0.47 ± 0.01**	**81.99 ± 8.53**
TorA-S191C ($-O_2^{ex}/+O_2^{pur}$)	**-0.43 ± 0.03**	**30.64 ± 1.96**
TorA-S191C ($+O_2^{ex}/+O_2^{pur}$)	**-**	**32.05 ± 3.53**
apo-TorA	**-**	**-**

[a]E_{onset} was determined using CV.
[b]MET is determined by measurement of the stationary reduction current after the addition of 3 mM TMAO to a solution containing 1 mM methyl viologen using amperometry at -0.8V.
[c](–) = no activity detected.

For table of contents use only

Modulating the molybdenum coordination sphere of *Escherichia coli* trimethylamine *N*-oxide reductase

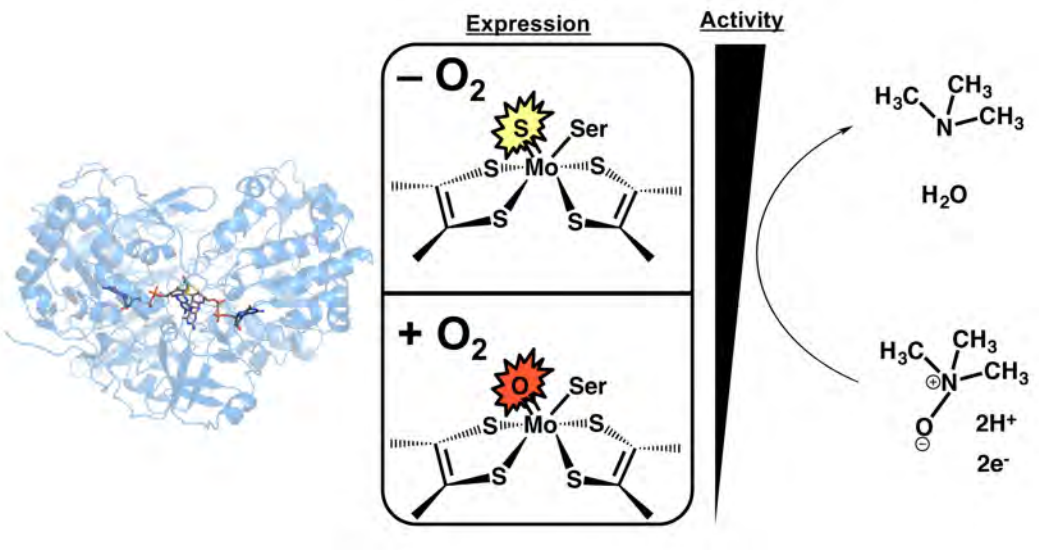

Supporting Information:

Modulating the molybdenum coordination sphere of Escherichia coli trimethylamine N-oxide reductase

Paul Kaufmann[1†], Benjamin R. Duffus[1†], Biljana Mitrova[1†], Chantal Iobbi-Nivol[2], Christian Teutloff[3], Manfred Nimtz[4], Lothar Jänsch[4], Ulla Wollenberger[1] and Silke Leimkühler[1*]

From the [1]Institute of Biochemistry and Biology, Department of Molecular Enzymology, University of Potsdam, 14476 Potsdam, Germany; [2]Aix-Marseille University, CNRS, BIP UMR7281, 13402 Marseille, France; [3]Institute for Experimental Physics, Free University of Berlin, Arnimallee 14, 14195 Berlin, Germany; [4]Helmholtz Center for Infection Research, Inhoffenstraße 7, 38124 Braunschweig, Germany.

***corresponding author:**

Silke Leimkühler; Department of Molecular Enzymology, Institute of Biochemistry and Biology, University of Potsdam, Karl-Liebknecht-Str. 24-25, 14476 Potsdam, Germany; Tel.: +49-331-977-5603; Fax: +49-331-977-5128; E-mail: sleim@uni-potsdam.de

†These authors contributed equally to this work

TABLE OF CONTENTS

Table S1: **TorA spin concentrations used in EPR spectroscopy.** The concentrations of TorA were determined by UV-visible absorption spectroscopy, while concentration of bound Mo was determined through ICP-OES. The spin concentrations were determined through use of the Matlab toolbox 'spincounting' from the obtained spectra and associated tune picture of the resonator. The reported percent spin relates the amount of spin to the amount of Mo present.

TorA treatment	TorA (μM)	Spin (μM)	Mo (μM)	% Spin
TorA-WT (Aerobic Expression/ Aerobic Purification)				
As-iso	356	4.5	121	3.7
DT-reduced	317	4.6	108	4.3
FeCN-oxidized	317	13.9	108	12.9
TorA-WT (Anaerobic Expression/Aerobic Purification)				
As-iso	128	4.8	124	3.8
DT-reduced	114	10.9	111	9.8
FeCN-oxidized	114	2.8	111	2.5
TorA-WT (Anaerobic Expression/ Anaerobic Purification)				
As-iso	129	3.8	124	3.1
DT-reduced	114	12.3	111	11.1
FeCN-oxidized	114	4.4	111	4.0
Redox-Cycled TorA-WT (Anaerobic Expression/Aerobic Purification)				
As-iso	225	0.8	90	0.9
DT-reduced	225	1.9	90	2.1
recTorA^{sulfido}bis-MGD^{FDH}				
As-iso	127	2.4	15.4	15.6
DT-reduced	114	2.6	13.9	18.7
recTorA^{sulfido}bis-MGD^{XDH}				
As-iso	138	1.8	4.6	39.1
DT-reduced	124	1.5	4.2	35.7
TorA^{S191C} (Anaerobic Expression/Aerobic Purification)				
As-iso	108	1.3	11.3	11.5

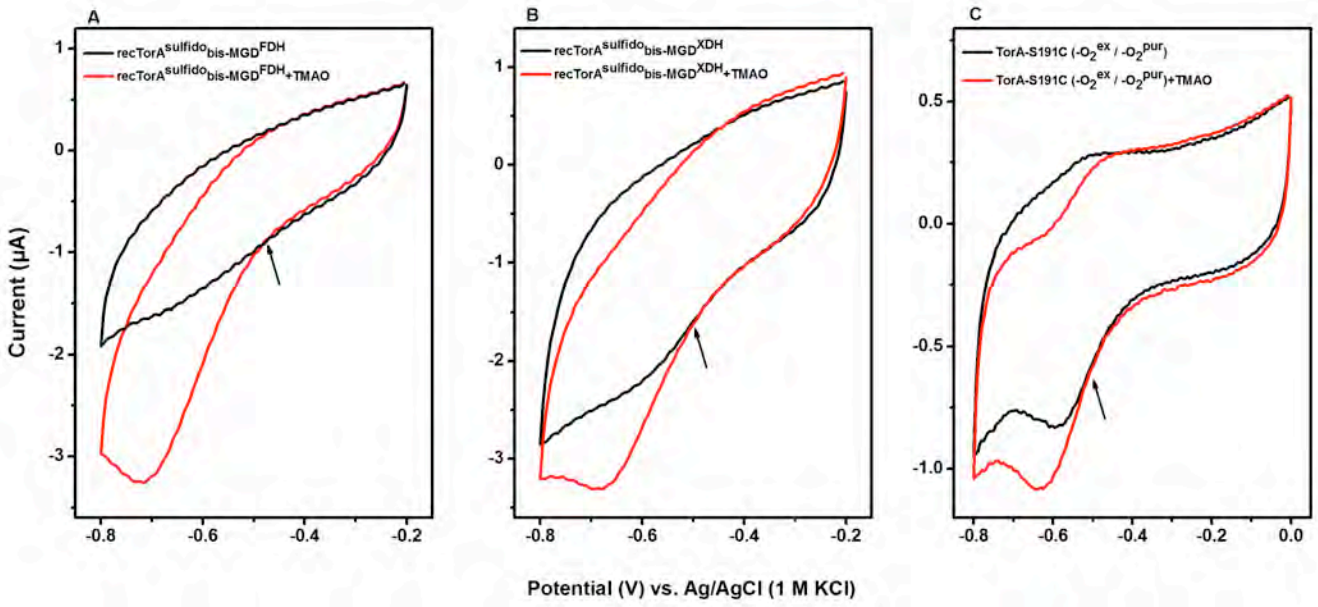

Figure S1: **Direct bioelectrocatalysis of active TorA variants with TMAO as substrate.** Direct bioelectrocatalysis of immobilized (A) recTorA^{sulfido}bis-MGD^{FDH} (B) recTorA^{sulfido}bis-MGD^{XDH} (C) TorA-S191C (-O_2^{ex} / -O_2^{pur}), with TMAO as substrate. The black traces show voltammograms recorded when no substrate is present and red traces measured in the presence of substrate in the measuring cell. The black arrow indicates the E_{onset}. Conditions: pH 6.5, 10 mM phosphate buffer, 3 mM TMAO, scan rate 5 mV/s, under stirring conditions.

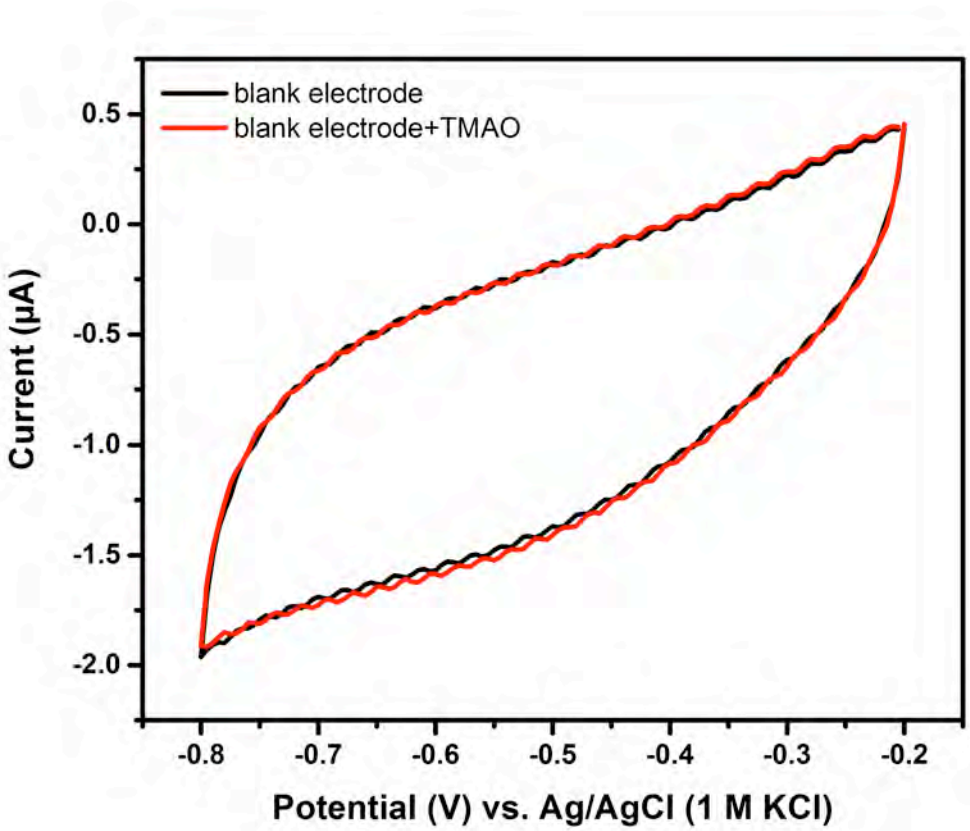

Figure S2: **Cyclic voltammogram of the blank electrode (no enzyme immobilized) in the presence and absence of TMAO.** The black traces show the voltammogram recorded when no substrate was present and the red traces were measured in the presence of substrate in the measuring cell. Conditions: pH 6.5, 10 mM phosphate buffer, 3 mM TMAO, scan rate 5 mV/s, under stirring conditions.

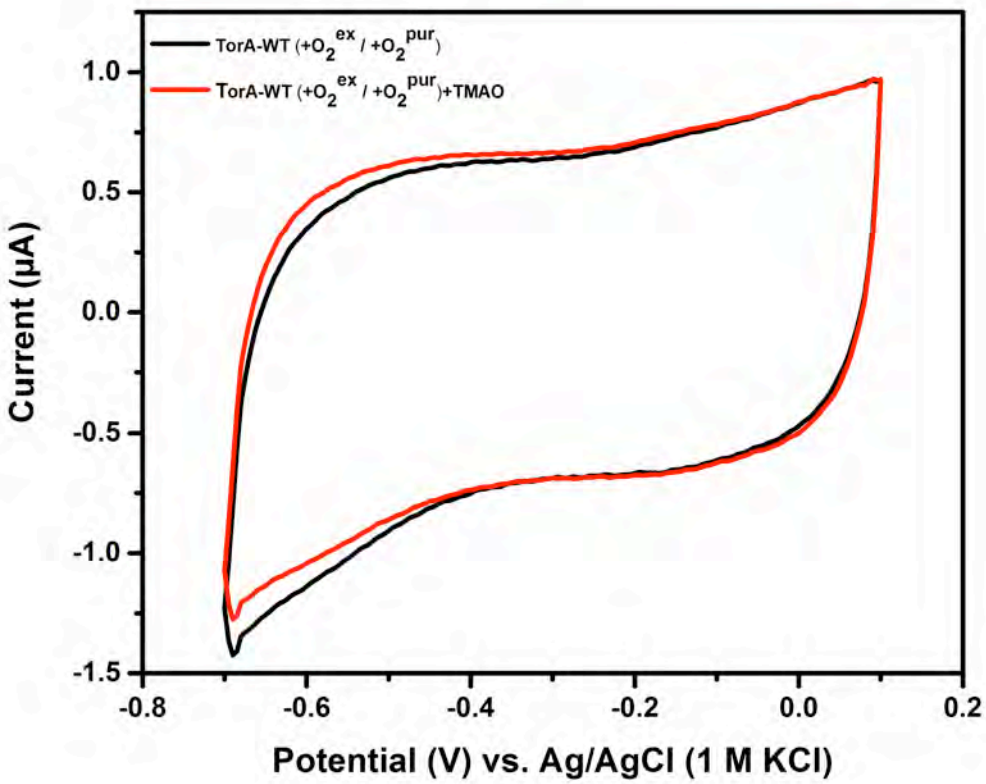

Figure S3**: Direct bioelectrocatalysis of immobilized aerobically expressed and purified TorA-WT with TMAO as substrate**. The black traces show the voltammogram recorded when no substrate was present and the red traces were measured in the presence of substrate in the measuring cell. Conditions: pH 6.5, 10 mM phosphate buffer, 3 mM TMAO, scan rate 5 mV/s, under stirring conditions.

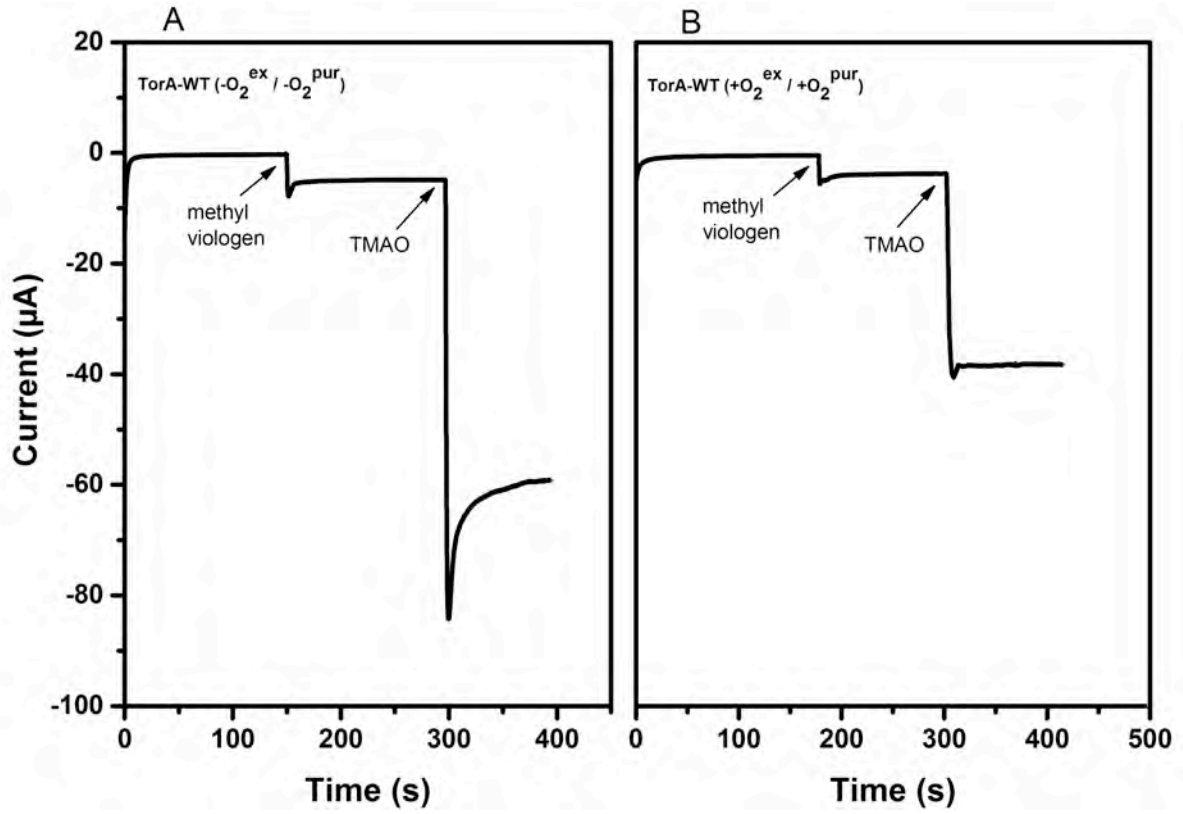

Figure S4: **Amperometric curves for mediated bioelectrocatalysis.**

(A) Immobilized TorA-WT anaerobically expressed and purified and (B) aerobically expressed and purified were measured in the presence of methyl viologen as mediator and TMAO as substrate. Conditions: pH 6.5, 10 mM phosphate buffer, 3 mM TMAO, 1 mM methyl viologen, potential applied -0.85 V, under stirring conditions.

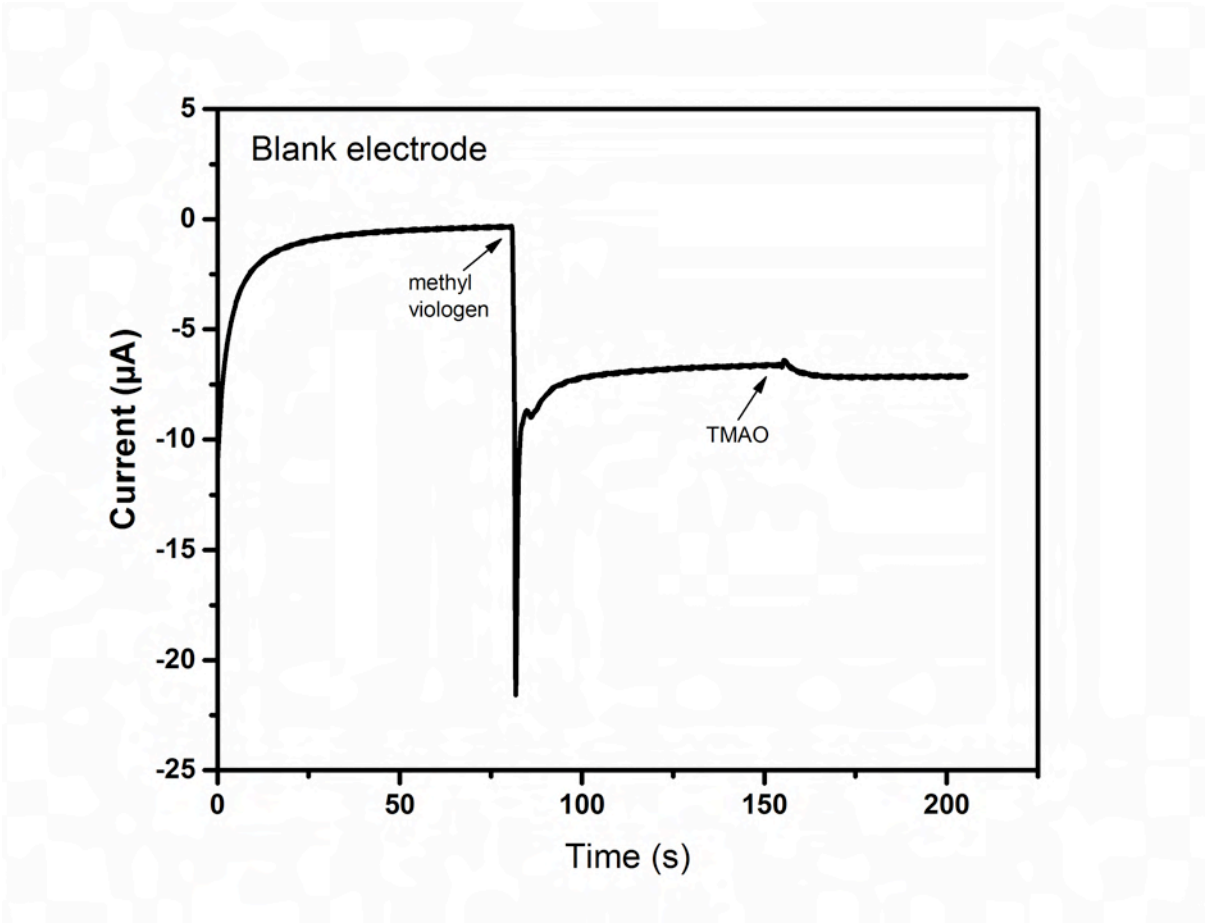

Figure S5: **Amperometric curves for the blank electrode.** The blank electrode (no enzyme immobilized) was measured in the presence of the mediator methyl viologen and TMAO. Conditions: pH 6.5, 10 mM phosphate buffer, 3 mM TMAO, 1 mM methyl viologen, potential applied -0.85 V, under stirring conditions.

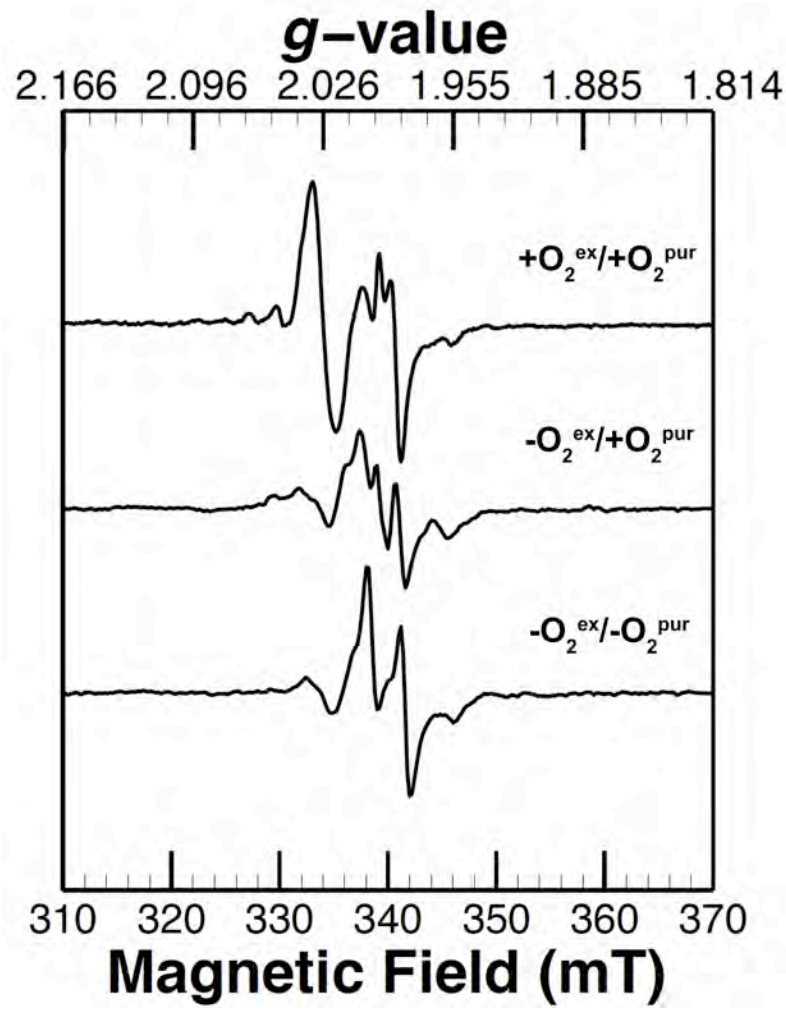

Figure S6: **Zoomed-in view of as-isolated TorA-WT EPR spectra.** Zoomed-in view of the spectra shown in Figure 8A-C (top traces) of TorA-WT prepared under different conditions. Spectra were obtained at 80 K with 3.93 mW microwave power, 5 G modulation amplitude and 100 kHz modulation frequency. Spectra were arbitrarily scaled to compare spectral lineshape.

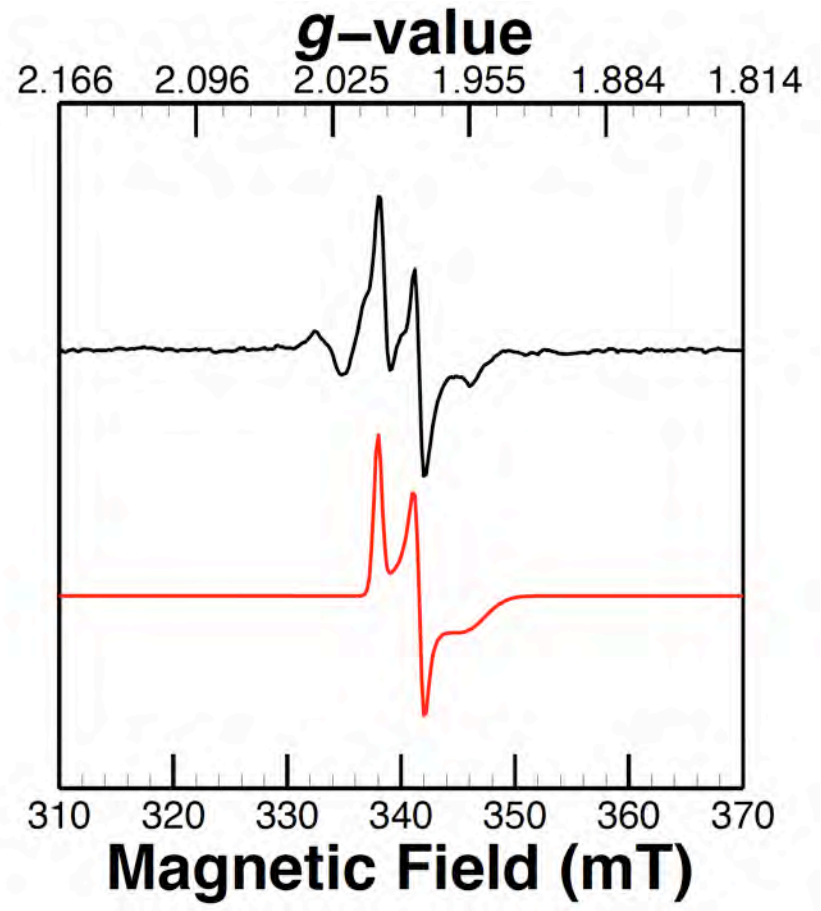

Figure S7: **EPR spectral simulation of TorA-WT (-O_2^{ex}/-O_2^{pur}) in the as-isolated state.** Experimental spectrum (black trace) represents the spectrum depicted in Figure 8C, top trace. Spectral simulation (red trace) was simulated as a one-component simulation, using the simulation toolbox EasySpin. Simulation parameters: *g:* 1.987, 1.965, 1.941 (g_{av} = 1.964, g_1-g_3 = 0.046), *g*-strain: 4.2, 4.2, 23.0 ($\times 10^{-3}$).

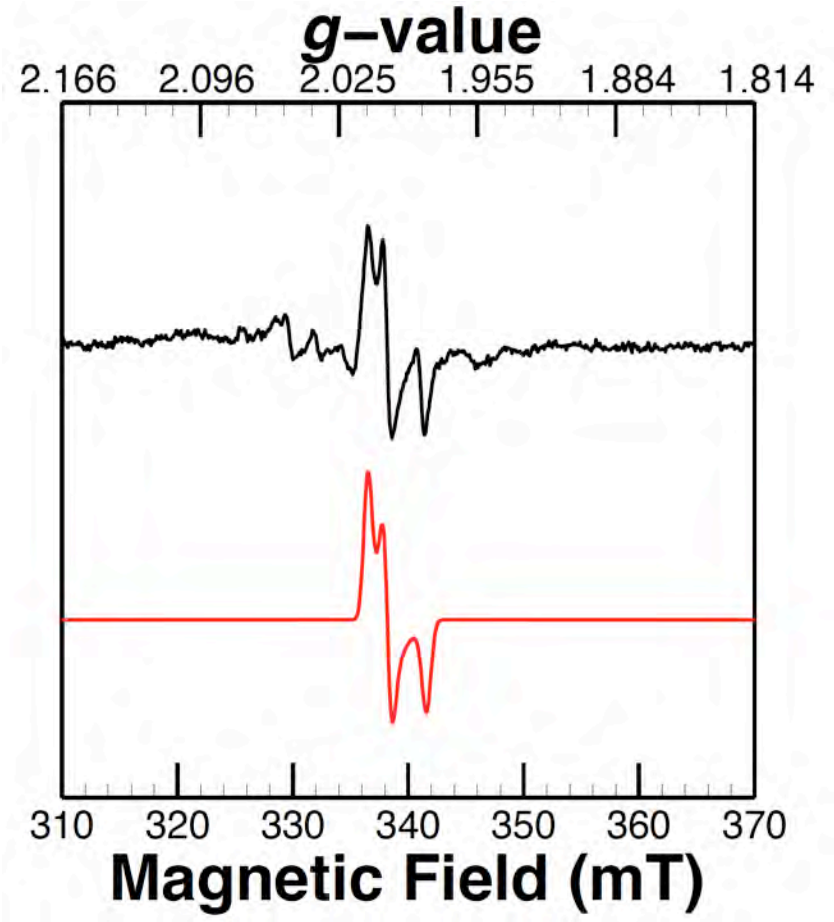

Figure S8: **EPR spectral simulation of recTorA^{sulfido}bis-MGD^{FDH} in the as-obtained state.** Experimental spectrum (black trace) represents the spectrum depicted in Figure 9A, bottom trace. Spectral simulation (red trace) was simulated as a one-component simulation, using the simulation toolbox EasySpin. Simulation parameters: *g*: 1.997, 1.986, 1.967 (g_{av} = 1.983, g_1-g_3 = 0.030), *g*-strain: 5.0, 4.0, 4.9 (X 10^{-3}).